Elements of Photonics, Volume I: In Free Space and Special Media. Keigo Iizuka
Copyright © 2002 John Wiley & Sons, Inc.
ISBNs: 0-471-83938-8 (Hardback); 0-471-22107-4 (Electronic)

ANSWERS TO PROBLEMS

Chapter 1

1.1 (a)

$$\mathbf{k} \cdot \mathbf{r} = 67.32$$
$$2\pi f = 2.44 \times 10^{15}$$
$$\mathbf{k} \cdot \mathbf{r} = \frac{2\pi}{\lambda}(x \sin\phi \cos\theta + y \sin\phi \sin\theta + z \cos\phi)$$

Hence, $\lambda = 0.497$ μm, where λ is the wavelength in the medium.

(b) The wavelength λ_a in air is found from

$$2\pi f = 2\pi \frac{c}{\lambda_a}$$

and $\lambda_a = 0.77$ μm. Thus,

$$n = \frac{\lambda_a}{\lambda} = \frac{0.772}{0.497} = 1.55$$

1.2 (a) We have

$$f_z = \sqrt{f_s^2 - f_x^2 - f_y^2} = \sqrt{\left(\frac{1}{0.84}\right)^2 - 0.6^2 - 0.8^2}$$
$$= 0.645 \quad \text{line/μm}$$

From Eq. (1.20)

$$e_x = \frac{f_x}{f_s} = 0.84 \times 0.6 = 0.504$$
$$e_y = \frac{f_y}{f_s} = 0.84 \times 0.8 = 0.672$$
$$e_z = \frac{f_z}{f_s} = (0.84)(0.65) = 0.55$$
$$e_x = \sin\phi \cos\theta = 0.504$$

$$e_y = \sin\phi \sin\theta = 0.672$$
$$e_z = \cos\phi = 0.545$$
$$\phi = 57^\circ \quad \text{and} \quad \theta = 53^\circ$$

(b) The angle θ between $\hat{\mathbf{e}}$ and $\hat{\mathbf{e}}_{\hat{\imath}}$ (see Fig. A1.2) is

$$\cos\theta = \hat{\mathbf{e}} \cdot \hat{\mathbf{e}}_{\hat{\imath}}$$

Hence, $\lambda_l \hat{\mathbf{e}} \cdot \hat{\mathbf{e}}_l = \lambda_s$.

$$0.84 = \lambda_l(\tfrac{3}{5}\mathbf{i} + \tfrac{4}{5}\mathbf{j})\cdot(0.504\mathbf{i} + 0.672\mathbf{j} + 0.55\mathbf{k}) = 0.84\lambda_l$$
$$f_l = \frac{1}{\lambda_l} = 1 \text{ line}/\mu\text{m}$$

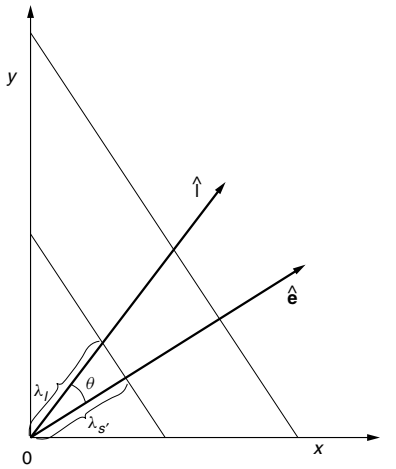

Figure A1.2 Wavelength measured along a line in the direction $\hat{\imath}$.

1.3 The Fourier transform of the input function is

$$\mathcal{F}\{t(x_0, y_0)\} = \iint_{-\infty}^{\infty} \left(1 + \frac{e^{j2f_{x0}x_0} + e^{-j2\pi f_{x0}x_0}}{2}\right) e^{-j2\pi f_x x_0} dx_0\, dy_0$$
$$= \left[\delta(f_x) + \tfrac{1}{2}\delta(f_x - f_{x0}) + \tfrac{1}{2}\delta(f_x + f_{x0})\right] \delta(f_y)$$

From Eq. (1.36), the diffraction pattern is

$$E(x_i, y_i) = \frac{e^{jk[z_i + (x_i^2 + y_i^2)/2z_i)]}}{j\lambda z_i} \left[\delta\left(\frac{x_i}{\lambda z_i}\right) + \frac{1}{2}\delta\left(\frac{x_i}{\lambda z_i} - f_{x0}\right) + \frac{1}{2}\delta\left(\frac{x_i}{\lambda z_i} + f_{x0}\right)\right] \delta\left(\frac{y_i}{\lambda z_i}\right)$$

The result is three peaks, as shown in Fig. A1.3.

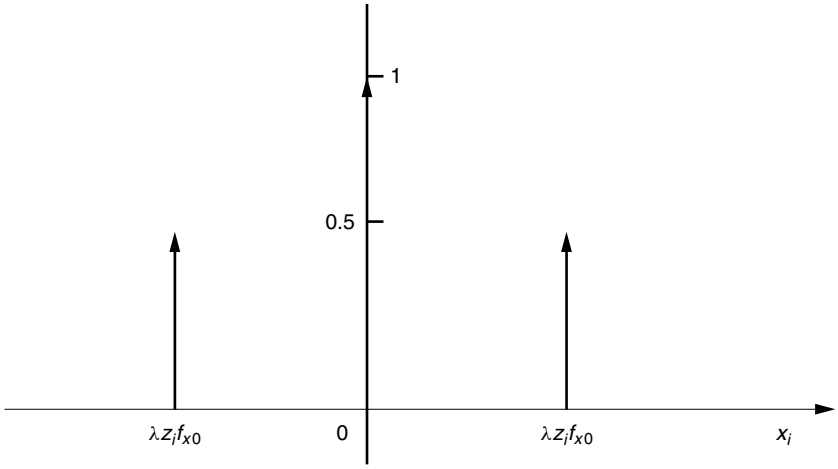

Figure A1.3 Diffraction pattern from the sinusoidal transmittance.

1.4 The current along the dipole antenna is expressed as

$$
\begin{aligned}
I(x_0) &= I_0 \cos\left(\frac{2\pi}{\lambda}x_0\right)\Pi\left(\frac{2x_0}{\lambda}\right) \\
\mathcal{F}\{I(x_0)\} &= \frac{\lambda}{4}I_0\left[\delta\left(f-\frac{1}{\lambda}\right)+\delta\left(f+\frac{1}{\lambda}\right)\right] * \text{ sinc }\left(\frac{\lambda}{2}f\right) \\
&= \frac{\lambda}{4}I_0\left[\text{sinc }\frac{\lambda}{2}\left(f-\frac{1}{\lambda}\right)+\text{sinc }\frac{\lambda}{2}\left(f+\frac{1}{\lambda}\right)\right] \\
&= \frac{\lambda}{2\pi}I_0\left[\frac{\sin\left(\frac{\pi}{2}\lambda f-\frac{\pi}{2}\right)}{(\lambda f-1)}+\frac{\sin\left(\frac{\pi}{2}\lambda f+\frac{\pi}{2}\right)}{(\lambda f+1)}\right]
\end{aligned}
$$

The radiation pattern of the antenna is

$$E_\theta = \frac{60}{j\lambda}\mathcal{F}\{I(x_0)\}_{f=(\cos\theta)/\lambda}\sin\theta$$

A few things should be noted about the result. There exist some differences in convention for expressing the same quantities (see Fig. A1.4). In antenna theory, the elevation angle θ is measured from the antenna axis rather than θ' from the normal to the antenna axis, and $f = (\cos\theta)/\lambda$ rather than $f = (\sin\theta)/\lambda$ is used. Also, the field E_θ of the θ component is used rather than the E_x component, and a factor $\sin\theta$ has to be multiplied. The final result is

$$E_\theta = -j60I_0\frac{\cos\left(\frac{\pi}{2}\cos\theta\right)}{\sin\theta}$$

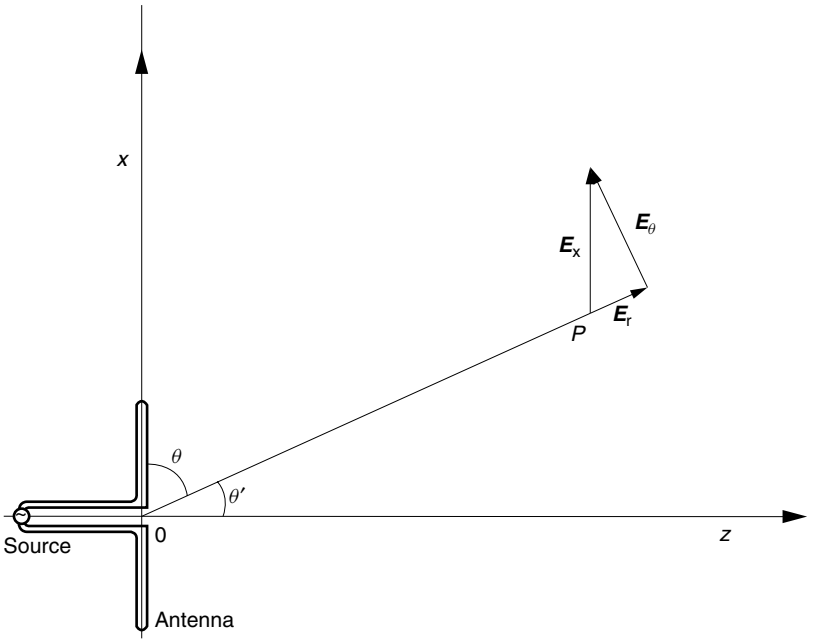

Figure A1.4 Field from a half-wave dipole antenna.

1.5

$$A-2, \quad B-1, \quad C-4, \quad D-3$$

1.6

$$A-4, \quad B-1, \quad C-2, \quad D-3$$

1.7 **(a)** The diffraction pattern at $z = z_i$ of the finite-sized lens is

$$E(x_i, y_i) = \frac{e^{jk[z_i+(x_i^2+y_i^2)/2z_i]}}{j\lambda z_i}\mathcal{F}\left\{ \underbrace{\Pi\left(\frac{x}{a}\right)\Pi\left(\frac{y}{a}\right)}_{\text{Aperture}} \times \underbrace{e^{-jk[(x^2+y^2)/2f_0]}}_{\text{Lens}} \underbrace{e^{jk[(x^2+y^2)/2z_i]}}_{\substack{\text{Part of point spread} \\ \text{function}}} \right\}_{f_x=x_i/\lambda z_i,\ f_y=y_i/\lambda z_i}$$

At the focal plane $z_i = f_0$ the last two factors cancel and

$$E(x_i, y_i) = \frac{e^{jk[f_0+(x_i^2+y_i^2)/2f_0]}}{j\lambda f_0}\ \text{sinc}\left(a\frac{x_i}{\lambda f_0}\right)\ \text{sinc}\left(a\frac{y_i}{\lambda f_0}\right)$$

The diffraction-limited main lobe spot size (zero crossing) is

$$\left(\frac{2\lambda f_0}{a}\right) \times \left(\frac{2\lambda f_0}{a}\right)$$

(b) $a = \dfrac{2\lambda f_0}{\Delta x} = \dfrac{2(0.555 \times 10^{-6}) + (50 \times 10^{-3})}{(1 \times 10^{-6})} = 55.5 \text{ mm}$

1.8 Figure P1.8 shows the geometry for taking a picture with a pinhole camera. For simplicity, only one point P_0 at $(l_0, 0, d_1)$ on the object is considered and the object is expressed by $\delta(x_0 - l_0)\delta(y_0)$. The aperture of the camera is in the x–y plane, which is d_1 away from the object. The aperture function is $\Pi(x/a)\Pi(y/a)$. The field that is illuminating the aperture is a spherical wave emanating from $(l_0, 0, d_1)$, and the field on the aperture is

$$E(x, y) = \frac{E_0}{j\lambda d_1} \exp\left[jk\left(d_1 + \frac{(x - l_0)^2 + y^2}{2d_1}\right)\right] \Pi\left(\frac{x}{a}\right) \Pi\left(\frac{y}{a}\right) \tag{1}$$

Before calculating the diffraction pattern of the field within the aperture, projected onto the film of the camera, some assumptions are made.

Assumption 1. The pinhole is made small such that the term with $x^2 + y^2$ in the exponent can be ignored, and $E(x, y)$ can be approximated as

$$E(x, y) \doteq \frac{E_0}{j\lambda d_1} e^{jk[d_1 + l_0^2/2d_1 - l_0 x/d_1]} \tag{2}$$

Using Eq. (1.38) again, the image on the film is calculated as

$$E(x_i, y_i) = \frac{-E_0}{\lambda^2 d_1 d_2} \exp\left[jk\left(d_1 + d_2 + \frac{l_0^2}{2d_1} + \frac{x_i^2 + y_i^2}{2d_2}\right)\right] \mathcal{F}\left\{e^{-jkl_0 x/d_1} \times \Pi\left(\frac{x}{a}\right) \Pi\left(\frac{y}{a}\right) e^{jk(x^2+y^2)/2d_2}\right\}_{f_x = x_i/\lambda d_2,\ f_y = y_i/\lambda d_2} \tag{3}$$

where d_2 is the length between the aperture and the film of the pinhole camera. An additional assumption is made.

Assumption 2. The limits of the Fourier transform integral of Eq. (3) are from $-a$ to a. The value of the exponent in the fourth term inside the Fourier transform is at most $ka^2/2d_2$, and the size $a \times a$ of the pinhole will be chosen so that this value is much smaller than unity.

With Assumption 2, Eq. (3) can be approximated as

$$E(x_i) = -\frac{E_0 a^2}{\lambda^2 d_1 d_2} \exp\left[jk\left(d_1 + d_2 + \frac{l_0^2}{d_1} + \frac{x_i^2 + y_i^2}{2d_2}\right)\right] \times \text{sinc}\left[a\left(\frac{l_0}{\lambda d_1} - \frac{x_i}{\lambda d_2}\right)\right] \text{sinc}\left(\frac{a y_i}{\lambda d_2}\right) \tag{4}$$

Thus, the image formed on the film is a sinc function centered at $(-l_0 d_2/d_1, 0)$ with the size of the main lobe of $2\lambda d_2/a$. Because of Assumption 2, this no longer holds true for larger values of a.

1.9 The output from lens L_1 is

$$E_1(x, y, f_1) = \frac{e^{jkf_1}}{j\lambda f_1} G\left(\frac{x}{\lambda f_1}, \frac{y}{\lambda f_1}\right)$$

which is the input to lens L_2. The output from lens L_2 is

$$\begin{aligned} E_2(x_i, y_i) &= \frac{e^{jk(f_1+f_2)}}{j\lambda f_2} \mathcal{F}\left\{\frac{1}{j\lambda f_1} G\left(\frac{x}{\lambda f_1}, \frac{y}{\lambda f_1}\right)\right\}_{f_x = x_i/\lambda f_2, f_y = y_i/\lambda f_2} \\ &= \frac{e^{jk(f_1+f_2)}}{j\lambda f_2} \frac{(\lambda f_1)^2}{j\lambda f_1} g\left(-\frac{\lambda f_1}{\lambda f_2} x_i, -\frac{\lambda f_1}{\lambda f_2} y_i\right) \\ E_2(x_i, y_i) &= -\frac{f_1}{f_2} e^{jk(f_1+f_2)} g\left(-\frac{f_1}{f_2} x_i, -\frac{f_1}{f_2} y_i\right) \end{aligned}$$

The output image is therefore f_2/f_1 times the input image and is inverted. The amplitude of the output image is $-f_2/f_1$ times that of the input image. The minus sign in the amplitude means the phase of the output light is reversed from that of the input, but human eyes, which are sensitive only to intensity, cannot recognize this. Recall that the magnified image from a single lens expressed by Eq. (1.151) has a quadratic phase factor. This quadratic phase factor can be eliminated with the two-lens arrangement.

1.10 **(a)** The case of the opaque dot: The field distribution at the back focal plane of lens L_2 is

$$\frac{e^{j2kf}}{j\lambda f_2}\left[\delta\left(\frac{x}{\lambda f_2}\right)\delta\left(\frac{y}{\lambda f_2}\right) + j\Phi\left(\frac{x}{\lambda f_2}, \frac{y}{\lambda f_2}\right)\right]$$

where

$$\Phi = \mathcal{F}\{\phi\}$$

With the opaque dot, the first term is removed. The second term is further Fourier transformed by L_3, and the field on the screen is

$$-e^{j4kf}\left(\frac{f_2}{f_3}\right) j\phi\left(-\frac{f_2}{f_3} x_i, -\frac{f_2}{f_3} y_i\right)$$

and the intensity pattern is

$$I_a(x_i, y_i) = \left(\frac{f_2}{f_3}\right)^2 \phi^2\left(-\frac{f_2}{f_3} x_i, -\frac{f_2}{f_3} y_i\right)$$

(b) The case of $\pi/2$-radian phase plate: The field distribution just after the phase plate in the back focal plane (x, y) of L_2 is

$$\frac{e^{j2kf}}{j\lambda f_2}\left[e^{j\pi/2}\delta\left(\frac{x}{\lambda f_2}\right)\delta\left(\frac{y}{\lambda f_2}\right)+j\Phi\left(\frac{x}{\lambda f_2},\frac{y}{\lambda f_2}\right)\right]$$

The field on the screen after the second lens L_3 is

$$-e^{j4kf}\frac{f_2}{f_3}\left[j+j\phi\left(-\frac{f_2}{f_3}x_i,-\frac{f_2}{f_3}y_i\right)\right]$$

The intensity distribution is

$$\begin{aligned}I_b(x_i y_i)&=\left(\frac{f_2}{f_3}\right)^2\left[1+\phi\left(-\frac{f_2}{f_3}x_i,-\frac{f_2}{f_3}y_i\right)\right]^2\\&\simeq\left(\frac{f_2}{f_3}\right)^2\left[1+2\phi\left(-\frac{f_2}{f_3}x_i,-\frac{f_2}{f_3}y_i\right)\right]\end{aligned}$$

(c) Comparing I_a and I_b: While case (a) provides ϕ^2, case (b) provides $1+2\phi$. The result of case (b) is linear with ϕ and a more truthful representation and more sensitive when $|\phi|^2<1$.

1.11 If the card of encryption is $n(x, y)$, that of decryption has to be $n^{-1}(-x,-y)$. The phase distribution of a convex lens is

$$n(x, y)=e^{-jk(x^2+y^2)/2f_0}$$

Thus

$$n^{-1}(-x,-y)=e^{jk(x^2+y^2)/2f_0}$$

which is the transmission coefficient of a concave lens of focal length f_0.

1.12

$$g(r,\theta)=\begin{cases}1 & b<r<a,\ \dfrac{\pi}{c}\le\theta\le\pi-\dfrac{\pi}{c},\ \text{and}\ \pi+\dfrac{\pi}{c}\le\theta\le 2\pi-\dfrac{\pi}{c}\\ 0 & \text{elsewhere}\end{cases}$$

$$\begin{aligned}g_n(r)&=\frac{1}{2\pi}\int_{\pi/c}^{\pi-\pi/c}g(r,\theta)e^{-jn\theta}\,d\theta+\frac{1}{2\pi}\int_{\pi+\pi/c}^{2\pi-\pi/c}g(r,\theta)e^{-jn\theta}\,d\theta\\&=\frac{-1}{n\pi}[1+(-1)^n]\sin\left(\frac{n\pi}{c}\right)\end{aligned}\tag{1}$$

$$g_n(r)=\begin{cases}1-\dfrac{2}{c} & n=0\\ -\dfrac{2}{n\pi}\sin\left(n\dfrac{\pi}{c}\right) & n=\text{even}\\ 0 & n=\text{odd}\end{cases}$$

The Fourier–Hankel transform is calculated from Eq. (1.61) and Eq. (1):

$$G(\rho, \phi) = 2\pi \left(1 - \frac{2}{c}\right) \int_0^a rJ_0(2\pi\rho r)\, dr - \sum_{\substack{n = -\infty \\ n = \text{even} \\ \text{except } n = 0}} (-j)^n e^{jn\phi} \left(\frac{4}{n}\right) \sin\left(\frac{n\pi}{c}\right) \int_b^a rJ_n(2\pi\rho r)\, dr$$

With the relationship

$$J_{-n}(x) = (-1)^n J_n(x)$$

$G(\rho, \phi)$ becomes

$$G(\rho, \phi) = 2\pi \left(1 - \frac{2}{c}\right) \int_0^a rJ_0(2\pi\rho r)\, dr + \sum_{m=1}^{\infty} (-1)^{m+1} \frac{4j}{m} \sin(2m\phi) \sin\left(2m\frac{\pi}{c}\right) \int_b^a J_{2m}(2\pi\rho r)\, dr$$

or

$$G(\rho, \phi) = \left(1 - \frac{2}{c}\right) \left(\frac{a}{\rho} J_1(2\pi\rho a) - \frac{b}{\rho} J_1(2\pi\rho b)\right) + \sum_{m=1}^{\infty} (-1)^{m+1} \frac{4j}{m} \sin(2m\phi) \sin\left(2m\frac{\pi}{c}\right) \int_b^a J_{2m}(2\pi\rho r)\, dr$$

For large c and small b, $G(\rho, \phi)$ approaches the value of a complete circular aperture.

1.13 The transmittance of the hologram is

$$t(x, y) = |O|^2 + |R|^2 + OR^* + O^*R \tag{1}$$

where t_0 and β are suppressed. According to the geometry for fabricating the hologram, the expressions for O and R are

$$O(x, y) = \frac{A}{j\lambda d_0} e^{jk[d_0 + (x^2 + y^2)/2d_0]} \tag{2}$$

$$R(x, y) = R_0 e^{-jkx \sin\theta} \tag{3}$$

According to the geometry for reconstructing the image, we can express the reconstruction beam P as

$$P(x, y) = P_0 e^{jkz} \tag{4}$$

Reconstruction of the virtual image is, from the third term of Eq. (1),

$$E_3(x_i, y_i) = AR_0P_0 \frac{e^{jk[z_i+d_0+(x_i^2+y_i^2)/2z_i]}}{j\lambda z_i} \frac{1}{j\lambda d_0} \times \mathcal{F}\left\{e^{jk(x^2+y^2)/2D} \cdot e^{jkx\sin\theta}\right\}_{f_x=x_i/\lambda z_i, f_y=y_i/\lambda z_i} \tag{5}$$

where

$$\frac{1}{D} = \frac{1}{d_0} + \frac{1}{z_i} \tag{6}$$

Using Eqs. (1.43) and (1.110), the result of the Fourier transform is

$$E_3(x_i, y_i) = AR_0P_0 \frac{e^{jk[z_i+d_0+(x_i^2+y_i^2)/2z_i]}}{j\lambda(z_i+d_0)} \cdot \left\{e^{-j\pi\lambda D[(f_x-\sin\theta/\lambda)^2+f_y^2]}\right\}_{f_x=x_i/\lambda z_i, f_y=y_i/\lambda z_i} \tag{7}$$

Insertion of $f_x = x_i/\lambda z_i$, $f_y = y_i/\lambda z_i$ provides

$$E_3(x_i, y_i) = AR_0P_0 \frac{e^{jk(z_i+d_0)}}{j\lambda(z_i+d_0)} \cdot \exp\left\{j\frac{k}{2}\left[\frac{x_i^2+y_i^2}{z_i}\left(1-\frac{D}{z_i}\right) + 2\frac{D}{z_i}x_i\sin\theta - D\sin^2\theta\right]\right\} \tag{8}$$

$$E_3(x_i, y_i) = \frac{AR_0P_0}{j\lambda(z_i+d_0)} \exp\left[jk\left((z_i+d_0) + \frac{1}{2(z_i+d_0)}[(x_i+d_0\sin\theta)^2 + y_i^2 - d_0(d_0+z_i)\sin^2\theta]\right)\right] \tag{9}$$

The last term in the exponent is an aberration term that is small when either $z_i \doteqdot -d_0$ or $\theta \doteqdot 0$. The virtual image is at a distance $z = z_i + d_0$ from the observer and is laterally shifted by $-d_0\sin\theta$ in the x_i direction.
Next, the real image is considered using the fourth term of Eq. (1):

$$E_4(x_i, y_i) = AR_0P_0 \frac{e^{jk[z_i-d_0+(x_i^2+y_i^2)/2z_i]}}{j\lambda z_i} \frac{1}{j\lambda d_0} \times \mathcal{F}\left\{e^{jk(x^2+y^2)/2D'} \cdot e^{-jkx\sin\theta}\right\}_{f_x=x_i/\lambda z_i, f_y=y_i/\lambda z_i} \tag{10}$$

where

$$\frac{1}{D'} = \frac{1}{z_i} - \frac{1}{d_0} \tag{11}$$

Replacing D by D' and $jkx\sin\theta$ by $-jkx\sin\theta$ in Eq. (8), $E_4(x_3, y_3)$ is obtained directly as

$$E_4(x_4, y_4) = \frac{AR_0P_0}{\lambda(z_i - d_0)} \exp\left[jk\left((z_i - d_0) + \frac{1}{2(z_i - d_0)}[(x_i + d_0\sin\theta)^2 + y_i^2 - d_0(d_0 - z_i)\sin^2\theta]\right)\right] \tag{12}$$

The results are summarized in Fig. A1.13.

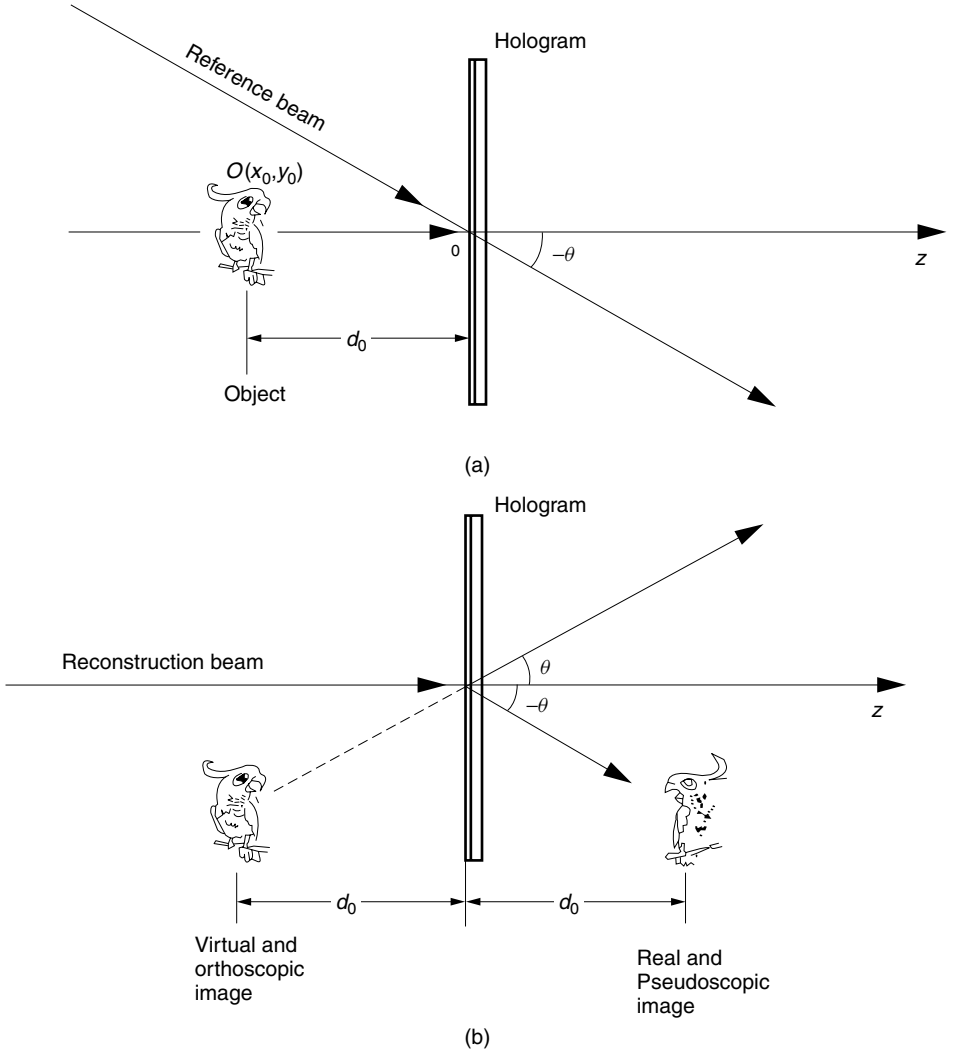

Figure A1.13 Location of the reconstructed images. (a) Fabrication of hologram. (b) Reconstructing the images.

Chapter 2

2.1 From Eqs. (2.2), (2.31), and (2.32),

$$\eta_1 H_1 \cos\theta_1 - \eta_1 H_3 \cos\theta_3 = \eta_2 H_2 \cos\theta_2 \tag{1}$$

$$H_1 + H_3 = H_2 \tag{2}$$

Equation (1) + Eq. (2) ($\eta_1 \cos\theta_3$) gives

$$\frac{H_2}{H_1} = \frac{2\eta_1 \cos\theta_1}{\eta_1 \cos\theta_1 + \eta_2 \cos\theta_2}$$

$$t_{\|H} = \frac{2n_2 \cos\theta_1}{n_2 \cos\theta_1 + n_1 \cos\theta_2} \neq t_{\|E}$$

Similarly, Eq. (1) − Eq. (2) ($\eta_2 \cos\theta_2$) gives

$$r_{\|H} = \frac{n_2 \cos\theta_1 - n_1 \cos\theta_2}{n_2 \cos\theta_1 + n_1 \cos\theta_2} = r_{\|E}$$

2.2 Snell's law changes Eq. (2.35) to

$$r_\| = \frac{E_3}{E_1} = \frac{\sin\theta_1 \cos\theta_1 - \sin\theta_2 \cos\theta_2}{\sin\theta_1 \cos\theta_1 + \sin\theta_2 \cos\theta_2}$$

which can be further rewritten as

$$\begin{aligned} r_\| &= \frac{\sin\theta_1 \cos\theta_1 (\cos^2\theta_2 + \sin^2\theta_2) - \sin\theta_2 \cos\theta_2 (\cos^2\theta_1 + \sin^2\theta_1)}{\sin\theta_1 \cos\theta_1 (\cos^2\theta_2 + \sin^2\theta_2) + \sin\theta_2 \cos\theta_2 (\cos^2\theta_1 + \sin^2\theta_1)} \\ &= \frac{(\cos\theta_1 \cos\theta_2 - \sin\theta_1 \sin\theta_2)(\sin\theta_1 \cos\theta_2 - \cos\theta_1 \sin\theta_2)}{(\sin\theta_1 \sin\theta_2 + \cos\theta_1 \cos\theta_2)(\cos\theta_1 \sin\theta_2 + \sin\theta_1 \cos\theta_2)} \\ &= \frac{\cos(\theta_1 + \theta_2)\sin(\theta_1 - \theta_2)}{\sin(\theta_1 + \theta_2)\cos(\theta_1 - \theta_2)} \end{aligned}$$

Thus,

$$r_\| = \frac{\tan(\theta_1 - \theta_2)}{\tan(\theta_1 + \theta_2)}$$

2.3 In the case of perpendicular polarization, E fields are parallel to the interface. They are identical with the tangential component of the field and $r_\perp + 1 = t_\perp$.

In the case of parallel polarization, the E field is not identical with the tangential component. Only a fraction of the E field is tangential to the interface. The tangential components satisfy the continuity condition while the E field itself does not. Hence, $r_\| + 1 \neq t_\|$ is true except in the case of normal incidence.

2.4 **(a)** From Eqs. (2.42) and (2.56), $R_\perp$ is

$$R_\perp = r_\perp^2 = \frac{\sin^2(\theta_1 - \theta_2)}{\sin^2(\theta_1 + \theta_2)} = \frac{(\sin\theta_1\cos\theta_2 - \cos\theta_1\sin\theta_2)^2}{\sin^2(\theta_1 + \theta_2)}$$

From Eqs. (2.44) and (2.55), $T_\perp$ is

$$T_\perp = \frac{n_2\cos\theta_2}{n_1\cos\theta_1} \cdot \frac{4\cos^2\theta_1\sin^2\theta_2}{\sin^2(\theta_1 + \theta_2)}$$

With Snell's law, $T_\perp$ is rewritten as

$$T_\perp = \frac{4\sin\theta_1\cos\theta_1\sin\theta_2\cos\theta_2}{\sin^2(\theta_1 + \theta_2)}$$

and hence,

$$R_\perp + T_\perp = 1$$

(b) From Eqs. (2.43) and (2.56), $R_\parallel$ is

$$R_\parallel = r_\parallel^2 = \frac{\tan^2(\theta_1 - \theta_2)}{\tan^2(\theta_1 + \theta_2)} = [\cos(\theta_1 + \theta_2)\sin(\theta_1 - \theta_2)]^2[\sin(\theta_1 + \theta_2)\cos(\theta_1 - \theta_2)]^{-2}$$

Thus,

$$R_\parallel = \frac{(\sin\theta_1\cos\theta_1 - \sin\theta_2\cos\theta_2)^2}{[\sin(\theta_1 + \theta_2)\cos(\theta_1 - \theta_2)]^2}$$

From Eqs. (2.45) and (2.55), $T_\parallel$ is

$$T_\parallel = \frac{n_2\cos\theta_2}{n_1\cos\theta_1}\left(\frac{2\cos\theta_1\sin\theta_2}{\sin(\theta_1 + \theta_2)\cos(\theta_1 - \theta_2)}\right)^2$$

With Snell's law, $T_\parallel$ is rewritten as

$$T_\parallel = \frac{4\sin\theta_1\cos\theta_1\sin\theta_2\cos\theta_2}{[\sin(\theta_1 + \theta_2)\cos(\theta_1 - \theta_2)]^2}$$

$$R_\parallel + T_\parallel = \frac{(\sin\theta_1\cos\theta_1 + \sin\theta_2\cos\theta_2)^2}{[\sin(\theta_1 + \theta_2)\cos(\theta_1 - \theta_2)]^2} = \frac{\left\{\frac{1}{2}(\sin 2\theta_1 + \sin 2\theta_2)\right\}^2}{[\sin(\theta_1 + \theta_2)\cos(\theta_1 - \theta_2)]^2} = \frac{[\sin(\theta_1 + \theta_2)\cos(\theta_1 - \theta_2)]^2}{[\sin(\theta_1 + \theta_2)\cos(\theta_1 - \theta_2)]^2} = 1$$

2.5 The condition for $r_\perp$ to be zero is $\theta_1 = \theta_2$, but due to Snell's law if $n_1 \neq n_2$, θ_1 can never be equal to θ_2.

2.6 When the angle of incidence is 57°, the light that is polarized in the plane of incidence is at Brewster's angle. Only the light that is polarized perpendicular to the plane of incidence (or perpendicular to the page) is reflected by G_1. The light then reaches G_2 resulting in l_0.

By rotating G_2 by 90° this light polarized perpendicular to the plane of incidence also satisfies Brewster's angle and is not reflected by G_2.

2.7

$$n_2 \sin\theta_1 = \sin\theta_2$$
$$n_x = n_2 \sin(90^\circ - \theta_1) = n_2 \cos\theta_1$$

Eliminate θ_1 from the above two equations to obtain

$$n_x = \sqrt{n_2^2 - \sin^2\theta_2}$$

Pulfrich's refractometer is widely used for measuring the index of refraction of fluid.

2.8

$$(n_1 k)^2 \cos^2\theta_1 - (n_2 k)^2 \cos^2\theta_2 = \left(n_1^2 - n_2^2\right) k^2$$
$$(n_1 k)^2 (1 - \sin^2\theta_1) - (n_2 k)^2 (1 - \sin^2\theta_2) = \left(n_1^2 - n_2^2\right) k^2$$

Thus,

$$k\left(n_1^2 \sin^2\theta_1 - n_2^2 \sin^2\theta_2\right) = 0$$

Chapter 3

3.1 The concentric fringe rings on the screen in Fig. 3.10 become blurred. The $x - z$ plane cross section of the cone shape is shown in Fig. A3.1.

3.2 Note from Eq. (3.66) that the measured quantity Δd_1 is augmented by m_1 times and the accuracy of the method in Section 3.4.3 is m_1 times higher than the method proposed in this problem.

3.3 From Eq. (3.70), $\Delta\lambda/\lambda$ is

$$\frac{\Delta\lambda}{\lambda} = \frac{\Delta d_2 - \Delta d_1}{d_2 - d_1} = \frac{0.1441 - 0.0829}{300}$$
$$= 2.040 \times 10^{-4}$$

The frequency of the He–Ne laser light is

$$\nu = \frac{c}{\lambda} = \frac{3 \times 10^{14}}{0.6328} = 4.741 \times 10^{14} \text{ Hz}$$

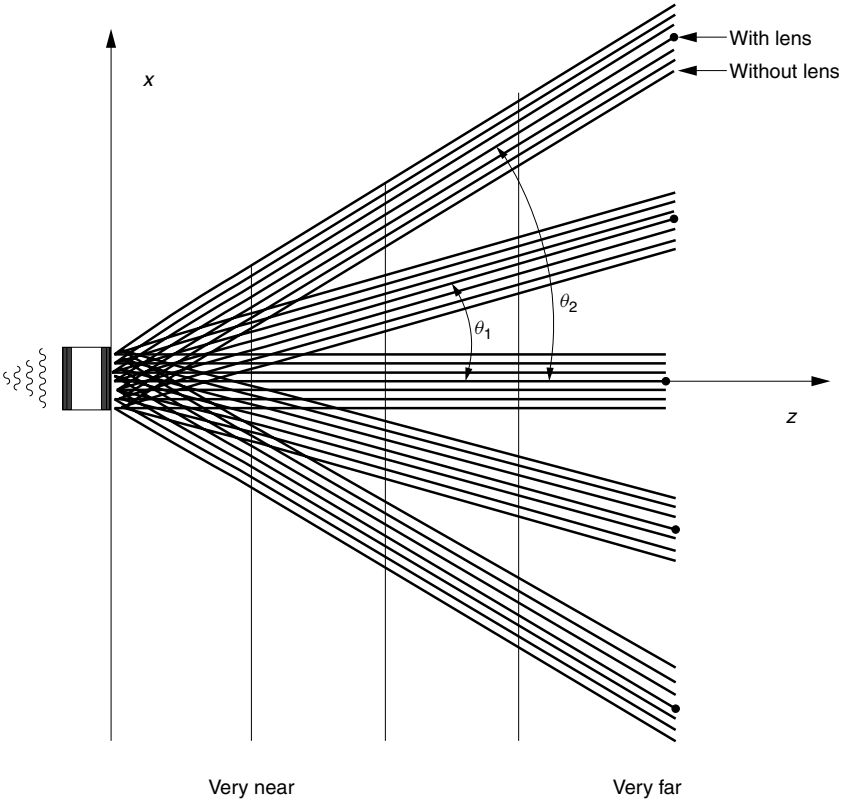

Figure A3.1 Solution of Problem 3.1.

Since

$$\frac{\Delta\nu}{\nu} = \frac{\Delta\lambda}{\lambda}$$

the modulation frequency is

$$\Delta\nu = \frac{\Delta\lambda}{\lambda}\nu = (2.040 \times 10^{-4})(4.741 \times 10^{14})$$
$$= 96.71 \text{ GHz}$$

3.4 (a)

$$d_{m+1} - d_m = \frac{\lambda}{2}$$
$$\lambda = 2(d_{m+1} - d_m) = 2(0.42) = 0.84 \text{ μm}$$

(b)

$$m\frac{\lambda}{2} = d$$
$$m = 2\frac{d}{\lambda} = \frac{2(420)}{0.84} = 1000$$

(c)

$$\begin{aligned}\Delta\nu &= \frac{d_1}{d_2}\Delta\nu_{\text{FSR}} \\ &= \frac{d_1}{d_2}\frac{c}{2d} = \frac{(0.1)(3\times 10^{14})}{(0.42)(2)(420)} \\ &= 85 \text{ GHz}\end{aligned}$$

3.5

$$\begin{aligned}r &= f\sin\theta_i \\ \theta_i &= \sin^{-1}\left(\frac{r}{f}\right) = \sin^{-1}\left(\frac{5.29}{50}\right) = 6.07^\circ \\ \sin\theta_i &= n_2\sin\theta = 1.05\sin\theta \\ \theta &= 5.78^\circ\end{aligned}$$

Note that

$$\begin{aligned}2n_2 d &= m\lambda \\ 2n_2 d\cos\theta &= (m-1)\lambda \\ \therefore\lambda &= 2n_2 d(1-\cos\theta) \\ &= 2(1.05)60(1-\cos 5.78^\circ) \\ &= 0.64\ \mu\text{m}\end{aligned}$$

3.6 The output intensity from the Fabry–Pérot cavity is, from Eq. (3.30) with $A = 0$,

$$I_t = I_0\frac{1}{1+M\sin^2\phi/2}$$

where

$$\phi = \frac{4\pi\nu}{c}d$$

At the resonance length

$$L = m\lambda/2$$

When the length of the cavity is enlongated by ΔL from the resonance length,

$$d = m\lambda/2 + \Delta L$$

ΔL that reduces the output to one-half of the value at the resonance is

$$\begin{aligned}1 &= M\sin^2\left[\frac{1}{2}\left(\frac{4\pi\nu}{c}\right)\left(m\frac{\lambda}{2}+\Delta L\right)\right] \\ &= M\sin^2\left(\frac{\pi}{\lambda}\Delta L\right)\end{aligned}$$

$$\Delta L \doteq \frac{\lambda}{\pi\sqrt{M}} = \frac{\lambda}{2}\frac{1}{F}$$

$$\frac{\Delta L}{L} = \frac{\lambda}{2FL} = \frac{1.064 \times 10^{-6}}{2(516)(300)} = 3.4 \times 10^{-12}$$

3.7 Using the parameters in Fig. A.3.7, $z_0/f = 0.5$. From Table 3.2 or from Figure A.3.7, $M = 1.8$, $W_1 = 0.18$ mm, $d_1 = 18$ cm, $z_1 = 160$ mm, and $\theta_1 = 0.063°$.

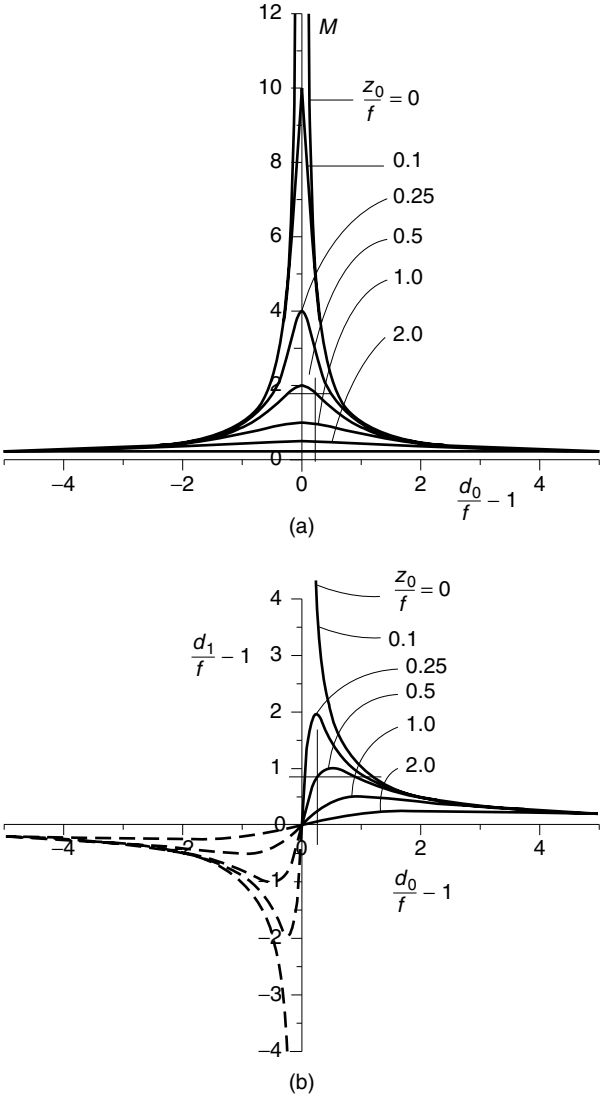

Figure A3.7 Values of M and $d_1/f - 1$ from the graphs.

3.8 **(a)** Using Eqs. (3.118) and (3.119), $(d_1 - f)$ in Eq. (3.117) is converted into $(d_0 - f)$, and $(d_0 - f)$ in the same equation is converted into $(d_1 - f)$; then the expression for d_0 in terms of f, d_1 and z_1 is

$$\begin{aligned} d_0 - f &= \frac{f^2(d_1 - f)}{(d_1 - f)^2 + z_1^2} \\ &= \frac{10^2(3.6 \times 10^6)}{(3.6 \times 10^6)^2 + \left[\left(\dfrac{\pi}{0.63 \times 10^{-6}}\right)(1)^2\right]^2} \\ &= 9.5\ \mu\text{m} \\ d_0 &= 10\ \text{m} + 9.5\ \mu\text{m} \end{aligned}$$

From Eqs. (3.116) and (3.118),

$$\begin{aligned} W_0 &= 1\sqrt{\frac{9.5 \times 10^{-6}}{3.6 \times 10^6}} \\ W_0 &= 1.62\ \mu\text{m} \end{aligned}$$

(b) When the distance is large compared to the beam waist, Eq. (3.106) and Fig. 3.25 give

$$\begin{aligned} \lim_{z \to \infty} \tan\theta &= \frac{2}{kW_0} \\ \frac{2}{kW_0} &\simeq \frac{1}{3.6 \times 10^6} \\ W_0 &\simeq \frac{3.6 \times 10^6}{\left(\dfrac{\pi}{0.63 \times 10^{-6}}\right)} \\ W_0 &\simeq 72\ \text{cm} \end{aligned}$$

3.9 If the beam is unfolded with respect to the plane mirror, then the problem becomes the same as the two concave mirror cavity with spacing $2d$ in place of d. From Eqs. (3.151) and (3.153),

$$\begin{aligned} W_1^2 &= \frac{2R_c}{k\sqrt{\dfrac{R_c}{d} - 1}} \\ W_0^2 &= \frac{2d}{k}\sqrt{\frac{R_c}{d} - 1} \end{aligned}$$

The same result can be obtained from the boundary conditions directly. Referring to Fig. P3.9 the phase of the waist matches that of the flat mirror. The flat mirror is placed at $z = 0$ or at the waist and the concave mirror is placed at $z = d$. At resonance, the radius of curvature R of the beam has to be matched with

the radius of curvature R_c of the mirror. The phase of the waist matches the flat mirror. Equation (3.100) gives the relationship among them. Insert W_0^2 of Eq. (3.100) into (3.96) to obtain

$$1 + \left(\frac{2R_c}{kW_1^2}\right)^2 = \frac{R_c}{d}$$

which leads to

$$W_1^2 = \frac{2R_c}{k\sqrt{\frac{R_c}{d} - 1}}$$

3.10 The propagation constant α is, from Eq. (3.171),

$$\alpha = k \sin\theta$$

The value of θ is determined by the size of the annular slit and the focal length as

$$\tan\theta = \frac{a}{f}$$

If θ is small, then $\sin\theta \doteqdot \tan\theta$ and from the above two equations

$$\alpha = 2\pi a/\lambda f$$

The first zero of the main lobe appears when

$$\alpha\rho = 2.4$$

and

$$\rho = 0.38\lambda f/a$$

Thus, the focal length f of the lens is

$$f = \frac{\rho a}{0.38\lambda} = \frac{(60 \times 10^{-6})(2.5 \times 10^{-3})}{(0.38)(0.63 \times 10^{-6})}$$
$$= 62.7 \text{ cm}$$

The radius R of the lens is, from Eq. (3.173),

$$R = z_{\max}\frac{a}{f} = (1)\frac{2.5 \times 10^{-3}}{(0.627)}$$
$$= 4.0 \text{ mm}$$

3.11 On the white side of the fin, a photon bounced off the surface changes its momentum from p to $-p$ and the amount of change in momentum is $2p$, while on the black side, the photon is absorbed and the change of the momentum is from p to 0 and the amount of change is p. It should rotate toward the black side of the fin. Crook's radiometer rotates in the opposite direction. It is propelled by the heat expansion of the gas on the black side.

3.12 When a photon collides, the momentum is changed from p to $-p$. The change of momentum is $2p$. From Eq. (3.199), the pushing force is

$$F = 2qn_1\frac{P}{c}$$

where q is the fraction of light effectively reflected back.

(a) $F = 2(0.07)(1.43)\dfrac{1}{3 \times 10^8} = 6.67 \times 10^{-10}$ newtons

(b) The mass of the sphere is

$$m = \tfrac{4}{3}\pi r^3 = \tfrac{4}{3}\pi(0.5145 \times 10^{-4}\text{ cm})^3 \times 10^{-3}$$
$$= 5.7 \times 10^{-16}\text{ kg}$$

The acceleration is

$$\frac{dv}{dt} = \frac{F}{m} = \frac{6.67 \times 10^{-10}}{5.7 \times 10^{-16}} = 1.17 \times 10^6\text{ m/s}^2$$

(c) The gravitational acceleration is

$$g = 9.8\text{ m/s}^2$$

The ratio is

$$\frac{dv/dt}{g} = 1.2 \times 10^5\text{ times}$$

3.13 As shown in Fig. A3.13, the direction is toward the focused beam.

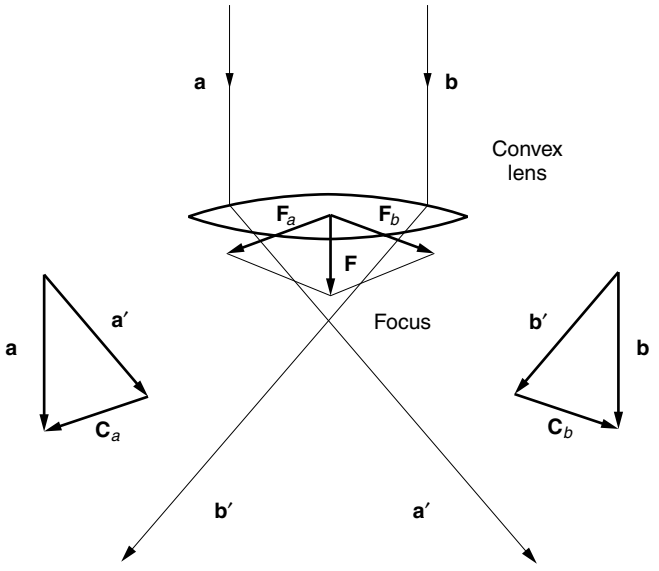

Figure A3.13 Laser radiation pressure on a convex lens.

Chapter 4

4.1 Inserting Eq. (4.61) into (4.62) gives

$$k_x^2\left(\frac{1}{n_o^2}-\frac{1}{n_e^2}\right)=0$$

(a) $k_x = 0$ together with the original assumption $k_y = 0$ means that the propagation vector **k** is along the z axis (or the optic axis).

(b) $n_o = n_e$ means that the medium is isotropic.

4.2

$$\begin{bmatrix} k_0^2n_\alpha^2-k_y^2-k_z^2 & k_xk_y & k_xk_z \\ k_yk_x & k_0^2n_\beta^2-k_x^2-k_z^2 & k_yk_z \\ k_zk_x & k_zk_y & k_0^2n_\gamma^2-k_x^2-k_y^2 \end{bmatrix}\begin{bmatrix} E_x \\ E_y \\ E_z \end{bmatrix}=0$$

where $k_0 = \omega/c$.

4.3 **(a)** The answer is given in Fig. A4.3a.

(b) The answer is given in Fig. A4.3b. It should be realized that the critical angle from the left is different from that from the right. There are two intersections

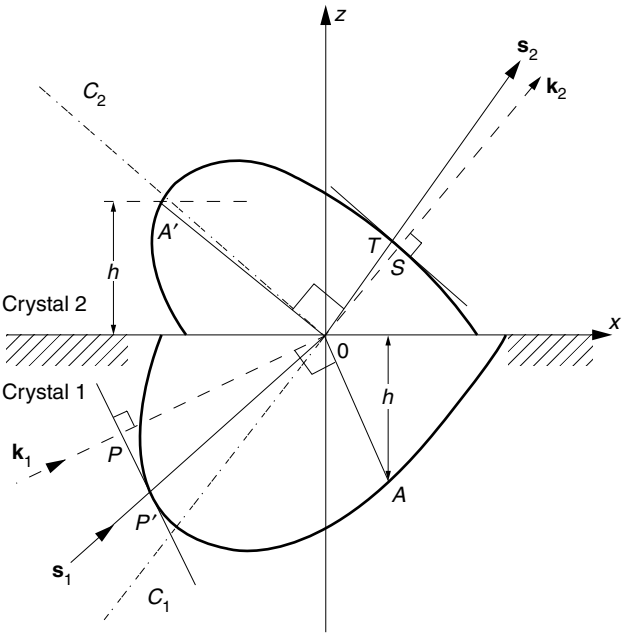

(a)

Figure A4.3 Answers to Problem 4.3. (a) Refraction at the boundary of uniaxial media. (b) The condition for total internal reflection at the boundary between uniaxial media. (c) Direction of the reflected ray.

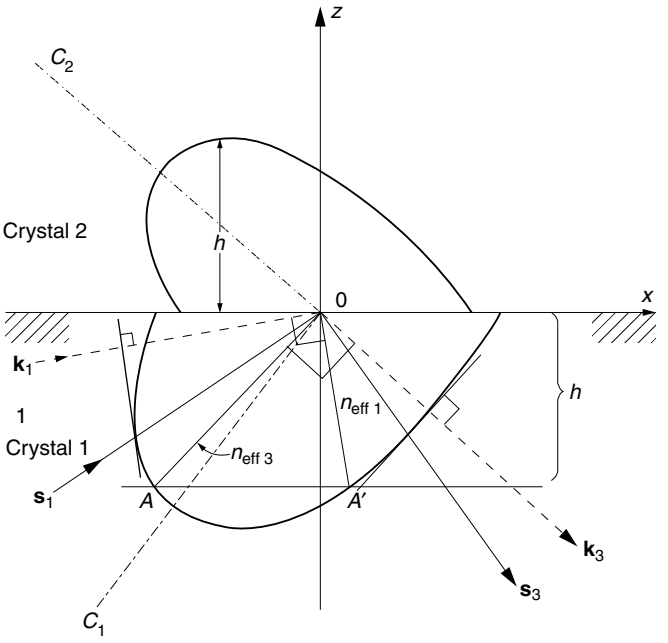

(b)

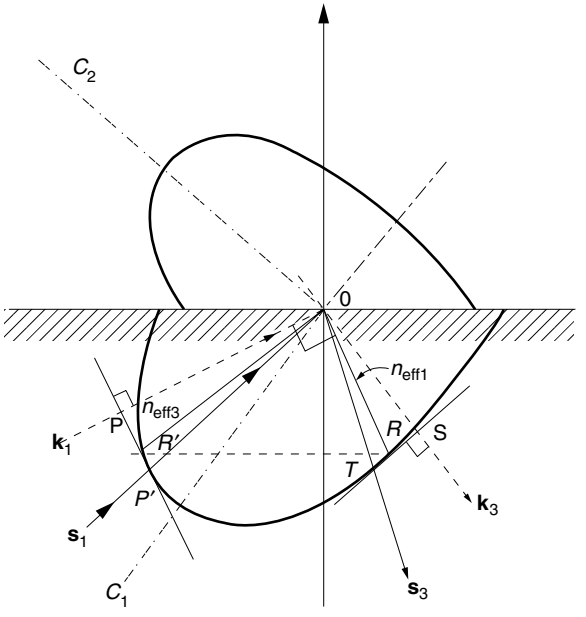

(c)

Figure A4.3 (*Continued*)

A and A' with the indicatrix, which are not symmetric with respect to the normal to the boundary, and the critical angle from the left side is different from that from the right.

(c) Referring to Fig. A4.3c, draw tangent $\overline{PP'}$ at P'. The line normal to $\overline{PP'}$ is $\mathbf{k}_1$. The line $\overline{0R}$, which is perpendicular to $\mathbf{k}_1$, represents n_{eff_1}. From R, line $\overline{RR'}$ is drawn parallel to the boundary until it intersects with the indicatrix at R'. $\overline{0R'}$ represents n_{eff_3}. The normal to $\overline{0R'}$ is $\mathbf{k}_3$. (Thus far, this discussion duplicates the discussion connected with Fig. 4.17.) The point of contact T to the indicatrix that the tangent $\overline{ST}$ makes determines the direction $\mathbf{s}_3$ of the reflected light ray.

4.4 The answer will be given by referring to Fig. A4.4. The critical angle ϕ_c^a between air and the $LiNbO_3$ interface is first calculated.

The point where the horizontal line a–a' at a distance $h = 1$ from the boundary intersects the ellipse determines n_{eff_3} at the critical angle. Equation (4.101) is used for calculating $n_{\text{eff}_3} = k/k_0$, but keep in mind that angle θ in Eq. (4.101) is the angle with respect to the optic axis of crystal. The optic axis of our crystal is horizontal. Put $\theta = 90^\circ + \theta_c$ and $h = n_{\text{eff}_3} \sin\theta_c$.

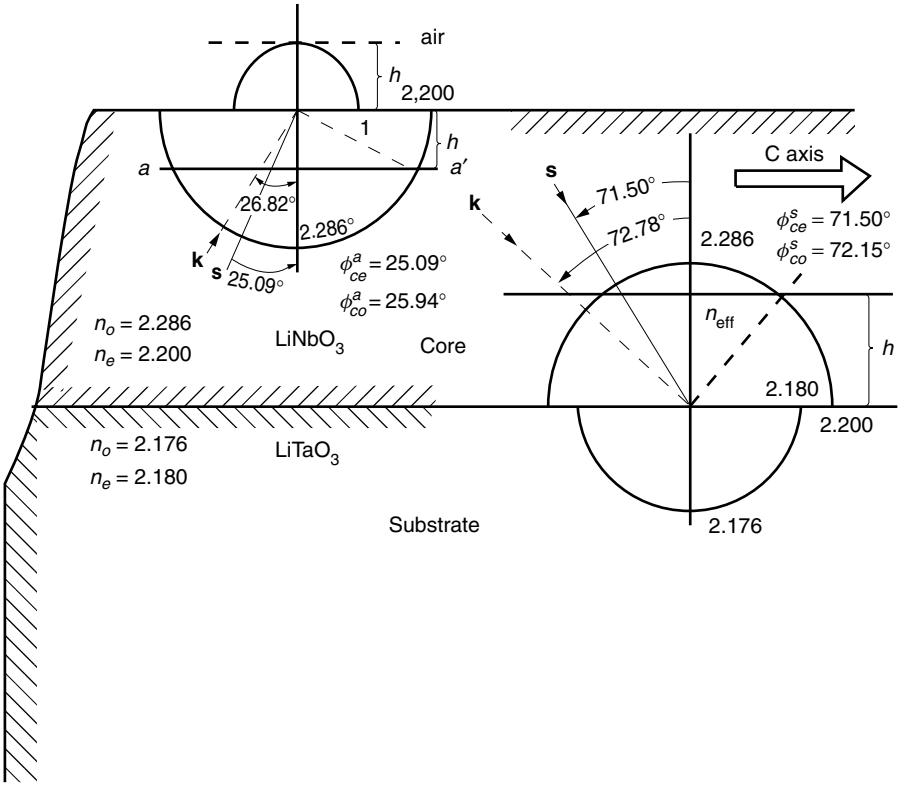

Figure A4.4 Examination of critical angles at the boundaries of an anisotropic optical guide.

$$h = \frac{\sin\theta_c}{\left[\left(\frac{\cos\theta_c}{n_e}\right)^2 + \left(\frac{\sin\theta_c}{n_o}\right)^2\right]^{1/2}}$$

which can be solved for $\sin\theta_c$ as

$$\sin\theta_c = \frac{h/n_e}{\left[1 + h^2\left(\frac{1}{n_e^2} - \frac{1}{n_o^2}\right)\right]^{1/2}}$$

Note that this expression is different from Eq. (4.112). Equation (4.112) applies when the crystal axis is normal to the interface. Inserting the given values, θ_c of the wavenormal at the critical angle is calculated as

$$\theta_c = 26.82^\circ$$

The direction ϕ of the light ray of the e-wave is obtained from Eq. (4.56). Again, the angles in Eq. (4.56) are with respect to the optic axis, which means $\theta = 26.82^\circ + 90^\circ$ and

$$\phi_{ce}^a = 25.09^\circ$$

where ϕ_{ce}^a is referred to the normal to the interface. The critical angle of the o-wave is simply

$$n_o \sin\phi_{co}^a = 1$$

and

$$\phi_{co}^a = 25.94^\circ$$

The difference in critical angle between the o- and e-waves is 0.88°.
Next, the critical angle between $LiNbO_3$ and $LiTaO_3$ is calculated. The maximum value of h associated with the interface is $h = 2.174$. Hence, θ_c from the above expression is

$$\theta_c = 72.78^\circ$$

Once again, the angles in Eq. (4.56) are with respect to the optic axis, which means that $\theta = 72.78^\circ + 90^\circ$. From Eq. (4.56), we find

$$\phi_{ce}^s = 71.50^\circ$$

where ϕ_{ce}^s is referred to the normal to the interface. The critical angle of the o-wave is

$$\sin\phi_{co}^s = \frac{2.176}{2.286}, \qquad \phi_{co}^s = 72.15^\circ$$

The difference in the critical angles between the o- and e-waves is 0.65°. The answers are summarized in Fig. A4.4.

4.5 **(a)** As shown in Fig. 4.12 as well as in Fig. A4.5a, by the time the wavefront of **D** reaches point P, the wavefront of **E** reaches point P'; thus,

$$v = u\cos\gamma \tag{1}$$

where v and u are the phase and ray velocities of the e-wave, respectively. γ is the angle between **s** and **k**, which is the same as that between **E** and **D**.

The left-hand side of Eq. (4.82) is the projection of **E** onto **D** and is rewritten as

$$E\cos\gamma = \left(\frac{v}{c}\right)^2 \frac{D}{\epsilon_0} \tag{2}$$

Inserting Eq. (1) into the right-hand side of Eq. (2) gives

$$\frac{D}{\epsilon_0 E}\cos\gamma = \left(\frac{c}{u}\right)^2 \tag{3}$$

With the relationship

$$\cos\gamma = \frac{\mathbf{E}\cdot\mathbf{D}}{ED} \tag{4}$$

Equation (4) is written as

$$\frac{n_o^2 E_x^2 + n_e^2 E_z^2}{E^2} = \left(\frac{c}{u}\right)^2 \tag{5}$$

where use was made of Eq. (3).

Note from Fig. A4.5a that

$$\frac{E_x}{E} = -\cos\phi, \qquad \frac{E_z}{E} = \sin\phi \tag{6}$$

$$\frac{\cos^2\phi}{v_o^2} + \frac{\sin^2\phi}{v_e^2} = \frac{1}{u^2} \tag{7}$$

where

$$v_o = \frac{c}{n_o}, \qquad v_e = \frac{c}{n_e} \tag{8}$$

Equation (7) is the expression for the ray velocity surface (suppressing the y components) and is called Huygens' wavelet ellipsoid. It provides the ray velocity for a given direction. The ray velocity for $\phi = 0$ or along the z direction is v_o, and that for $\phi = 90^\circ$ or along the x direction is v_e. In other words, when the wave propagates along the z axis, **D** is in the x direction and sees the index of refraction n_o; and when the wave propagates along the x axis, **D** is in the z direction and sees the index of refraction n_e. The index of refraction is determined by what **D** sees.

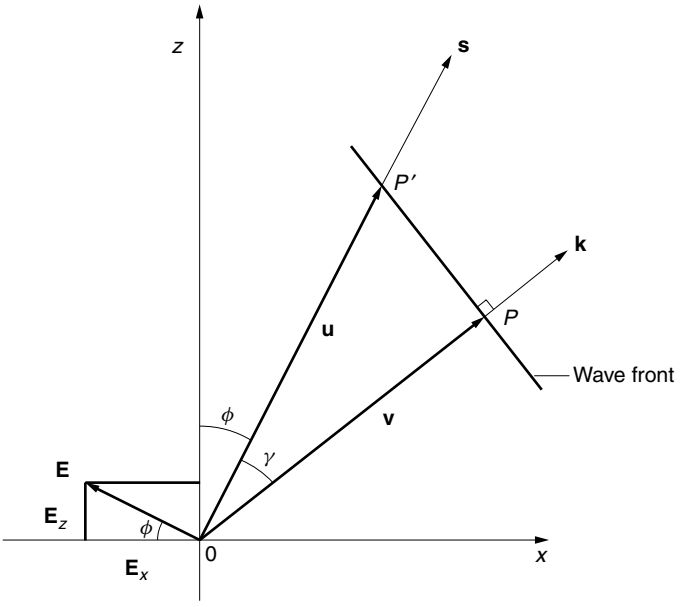

(a)

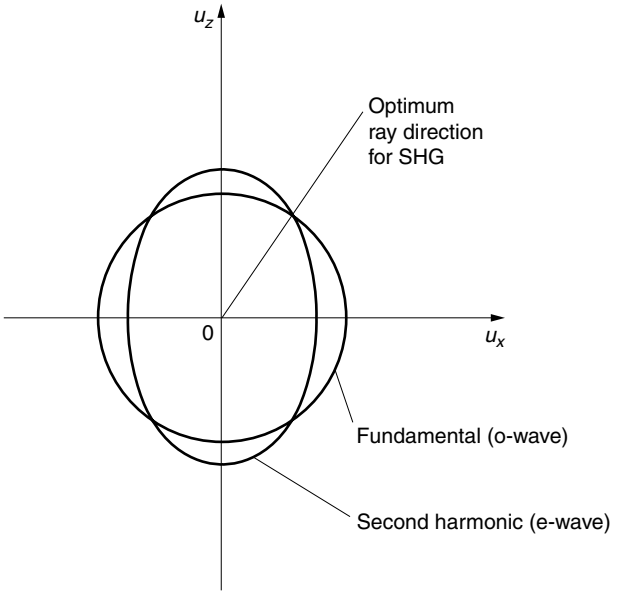

(b)

Figure A4.5 (a) Phase velocity **v** and ray velocity **u** of the e-wave. (b) Ray velocity matching for SHG.

Equation (7) immediately provides an expression for the wavelet spread in terms of spatial coordinates. Multiplying Eq. (7) by the distance r from the origin to the point of observation gives

$$\left(\frac{x}{v_e}\right)^2 + \left(\frac{z}{v_o}\right)^2 = t^2 \tag{9}$$

Equation (9) is the expression for an ellipse whose x axis is $v_e t$ and z axis is $v_o t$, both of which expand with t.

(b) As shown in Fig. A4.5b, the ray velocity diagram of the fundamental wave (o-wave) is overlayed with that of the second harmonic (e-wave). The intersection of the two diagrams is the optimum ray velocity direction for the SHG.

4.6 As the direction of the propagation is tilted from the z axis in the $x - z$ plane, the length of the major axis $\overline{0P}$ of the elliptic cross section moves along the circumference of the ellipse made with $y = 0$ in Eq. (4.84). $\overline{0P}$ of such an ellipse can be found by replacing

$$x = r\cos\theta$$
$$z = r\sin\theta$$
$$y = 0$$

in Eq. (4.84):

$$\left(\frac{\cos\theta}{n_\alpha}\right)^2 + \left(\frac{\sin\theta}{n_\gamma}\right)^2 = \frac{1}{r^2}$$

The angle θ is obtained by inserting

$$r = n_\beta$$

A method for experimentally finding the optical axes can be found in Ref. 15 in Chapter 4.

Chapter 5

5.1 It is seen from Eq. (5.10) that with $\varepsilon = \varepsilon_z$ one can take advantage of the large r_{33} of lithium niobate. The equation of the indicatrix, Eq. (5.4), becomes

$$\left(\frac{1}{n_o^2} + r_{13}\varepsilon_z\right)x^2 + \left(\frac{1}{n_o^2} + r_{13}\varepsilon_z\right)y^2 + \left(\frac{1}{n_e^2} + r_{33}\varepsilon_z\right)z^2 = 1$$

which can be approximated as

$$\frac{x^2}{(n_o - \frac{1}{2}r_{13}n_o^3\varepsilon_z)^2} + \frac{y^2}{\left(n_o - \frac{1}{2}r_{13}n_o^3\varepsilon_z\right)^2} + \frac{z^2}{\left(n_e - \frac{1}{2}r_{33}n_e^3\varepsilon_z\right)^2} = 1$$

Maximum retardation is achieved when light propagates in the $x - y$ plane. The amount of retardation is similar for any propagation direction in the $x - y$ plane.

For $k = k_y$,

$$\Delta = \frac{2\pi}{\lambda}(n_e - n_o)\, d + \frac{\pi}{\lambda}\left(n_o^3 r_{13} - n_e^3 r_{33}\right)\frac{V}{h}\, d$$

The first term is independent of the applied dc field and is called the *natural birefringence*, whereas the second term is the *induced birefringence*.

5.2 The linear portion of the I versus Δ curve is located at the point where $dI/d\Delta$ is constant. Therefore, the good biasing point is where $d^2I/d^2\Delta = 0$ is satisfied. Insertion of Eq. (5.29) into this equation leads to

$$\Delta_b = \frac{\pi}{2}$$

The retardance Δ is the sum of the bias term Δ_b and the modulated term Δ_m:

$$\Delta = \frac{\pi}{2} + \Delta_m$$

With the assumption that Δ_m is much smaller than $\pi/2$, and using the trigonometric relationship $\sin^2 A = \frac{1}{2}(1 - \cos 2A)$, Eq. (5.29) is approximated as

$$I = \frac{I_0}{2}(1 + \Delta_m)$$

where

$$\Delta_m = -\frac{2\pi}{\lambda}\left(r_{22} n_o^3 \varepsilon_m \cos \omega_m t\right) h$$

5.3 From Eq. (5.10) and $\varepsilon = (\varepsilon_x, \varepsilon_y, 0)$, the expression of the indicatrix is obtained. Since the direction of the propagation is along the z direction, the cross-sectional ellipse is

$$\left(\frac{1}{n_o^2} - r_{22}\varepsilon_y\right)x^2 + \left(\frac{1}{n_o^2} + r_{22}\varepsilon_y\right)y^2 - 2r_{22}\varepsilon_x xy = 1$$

The major and minor axes of this expression are immediately obtained by using the results of Example 5.4. Insertion of

$$A = \frac{1}{n^2} - r_{22}\varepsilon_y$$

$$C = \frac{1}{n^2} + r_{22}\varepsilon_y$$

$$B = -r_{22}\varepsilon_x$$

into Eq. (5.35) gives

$$\tan 2\theta = \frac{\varepsilon_x}{\varepsilon_y}$$

Let Φ be the angle between the resultant electric field and the x axis. Then Φ is expressed in terms of ε_x and ε_y as $\cot \Phi = \varepsilon_x/\varepsilon_y$. Using the identity

$$\cot \Phi = \tan\left(\frac{\pi}{2} - \Phi\right)$$

θ becomes

$$\theta = \frac{\pi}{4} - \frac{\Phi}{2}$$

If the external field is a rotating field at $\Phi = \Omega t$, the axis of the ellipse rotates in the opposite direction at one-half of the angular velocity Ω:

$$\theta = \frac{\pi}{4} - \frac{\Omega}{2}t$$

This fact is used for building a frequency shifter.

5.4 The two beams are

$$R = R_0 e^{j(k_x x + k_z z + \psi)}$$
$$S = S_0 e^{j(-k_x x + k_z z)}$$

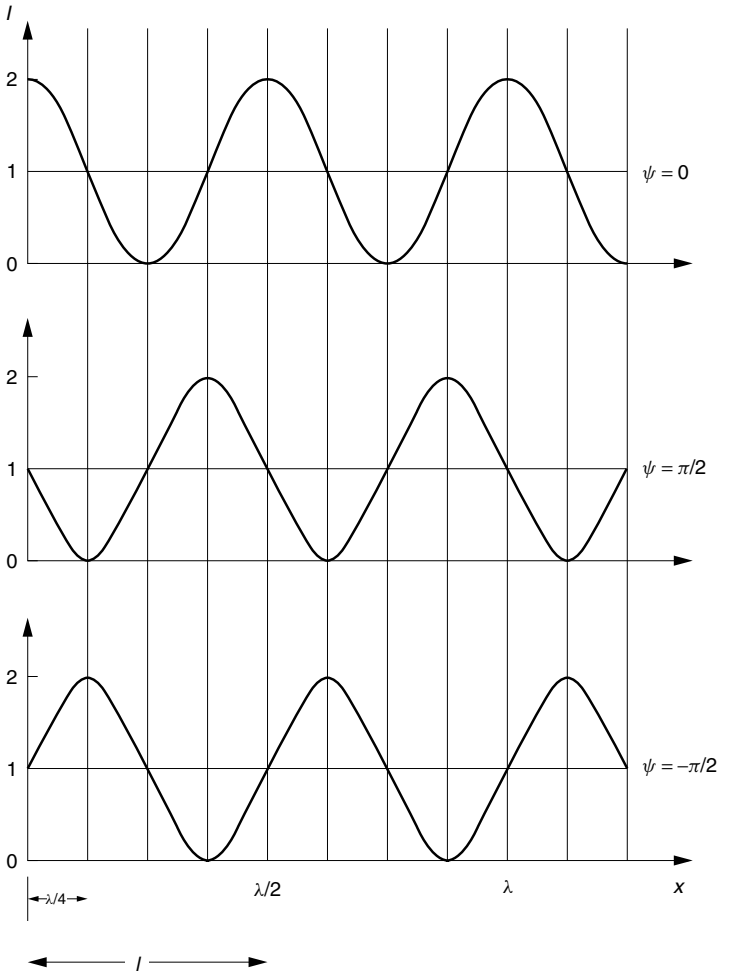

Figure A5.4 Intensity distributions $I = 2[1 + \cos(2k_x x + \psi)]$ for $\psi = 0, \pi/2, -\pi/2$ radians.

With $R_0 = S_0 = 1$, the fields on the $z = 0$ plane are found:

$$R + S = e^{j\psi/2}(e^{j(k_x x + \psi/2)} + e^{-j(k_x x + \psi/2)})$$
$$= 2e^{j\psi/2}\cos(k_x x + \psi/2)$$
$$|R + S|^2 = 4\cos^2(k_x x + \psi/2)$$
$$I = 2[1 + \cos(2k_x x + \psi)]$$

The intensity distributions for $\psi = 0, \pi/2, -\pi/2$ are shown in Fig. A5.4.

5.5 Extending the vector diagram in Fig. 5.21 to the case where $\psi = -\pi/2$, one finds that energy transfers from $S(x)$ to $R(x)$.

5.6 See Fig. A5.6.

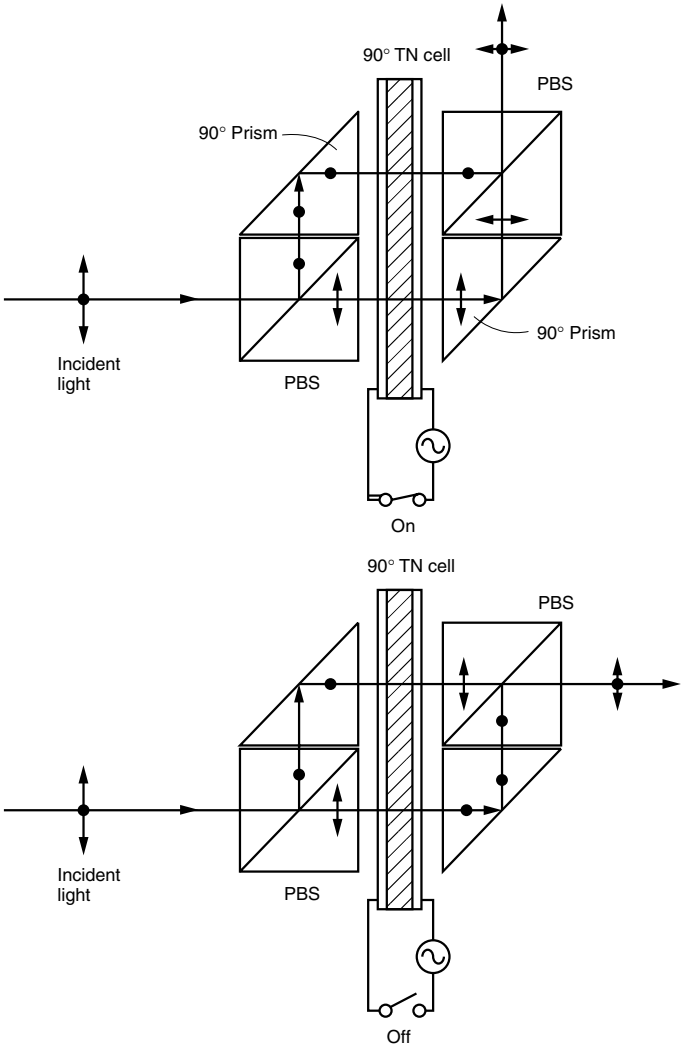

Figure A5.6 Light paths when the switch is on and off.

Chapter 6

6.1 Let

$$E_- = e^{-j\omega t + j\beta z}$$

$$E_+ = e^{j\omega t - j\beta z}$$

Let the plane of observation be $z = 0$. The phasor circles C_1 and C_2 of E_- rotate clockwise, while those of E_+ rotate counterclockwise. The 90° phase delay of the retarder is represented by

$$E_{-y} = e^{-j\omega t + j90^\circ}$$

$$E_{+y} = e^{j\omega t - j90^\circ}$$

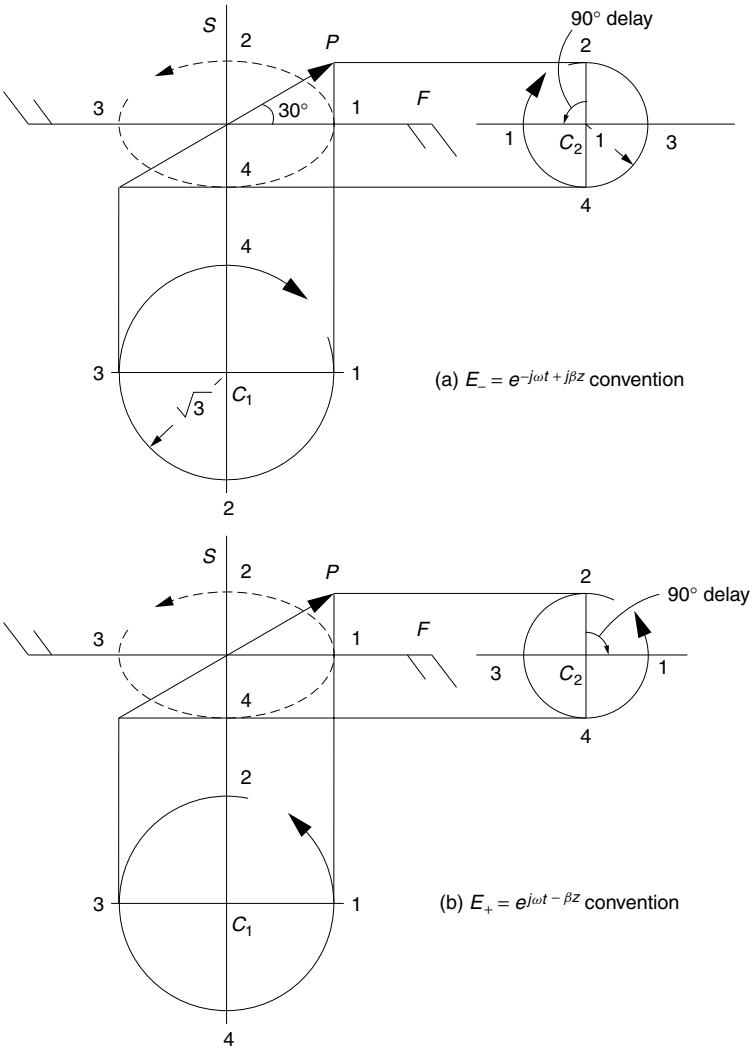

Figure A6.1 A difference in convention does not affect the final results.

The ellipses using these two different conventions are drawn in Fig. A6.1. The same final results are obtained.

6.2 The solution is obtained by the circle diagram as shown in Fig A6.2. From the diagram

$$\theta_2 = 68^\circ \quad \text{and} \quad \epsilon = 0.31$$

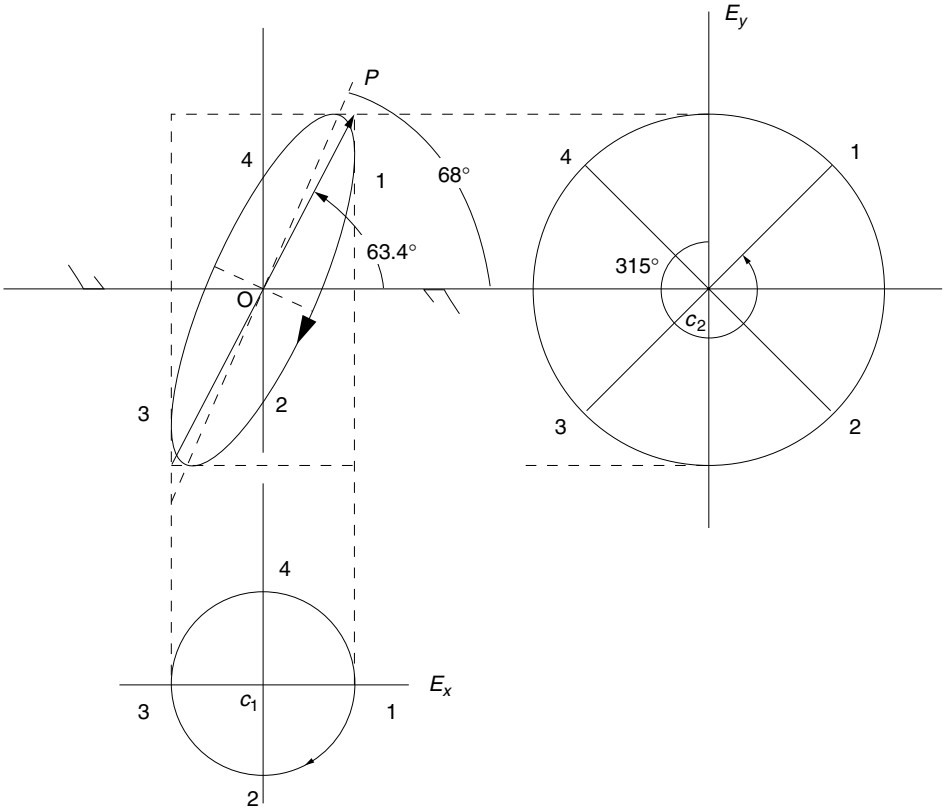

Figure A6.2 Circle diagram with $\theta_1 = 63.4^\circ (B/A = 2)$ and $\Delta = 315^\circ$.

6.3 The results are summarized in Fig. A6.3. As expected from the answer of Example 6.1, the major or minor axis is always along the fast axis, which is a characteristic of the combination of a linearly polarized wave and the quarter-waveplate.

When E_x and E_y of the incident linear polarization have the same sign, the result is left-handed rotation or counterclockwise rotation, whereas when E_x and E_y have opposite signs, the result is right-handed or clockwise rotation, as summarized in Fig. A6.3b.

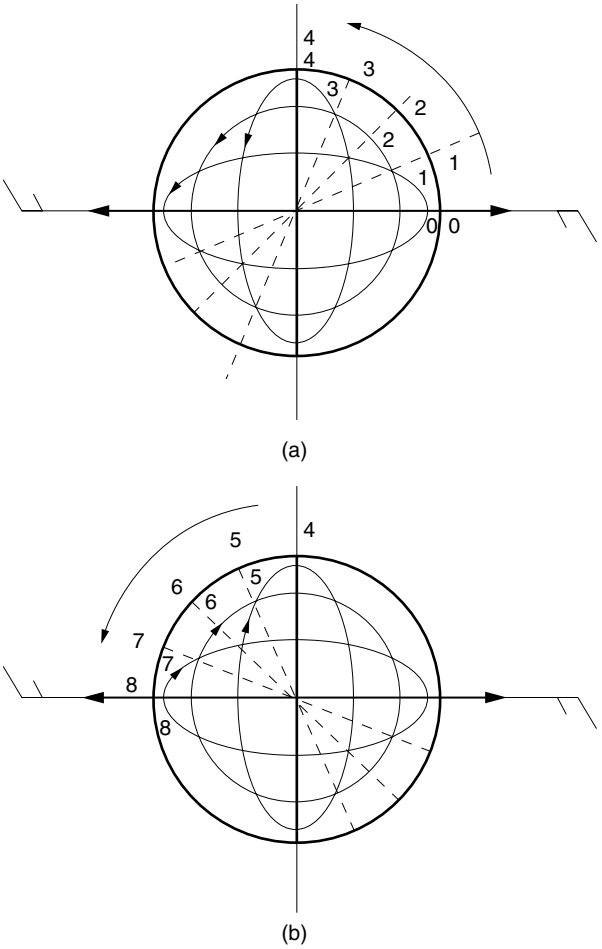

Figure A6.3 Transitions of the state of polarization as the azimuth of the incident linearly polarized wave is rotated. The fast axis of the $\lambda/4$ plate is along the x direction.

6.4 Referring to Fig. A6.4, point 1 on the major axis of the ellipse corresponds to the 1's on the circles C_1 and C_2. The phasor of C_2 is delayed from that of C_1 by 90°.

6.5 The result by the circle diagram method is shown in the dotted line in Fig. A6.5. The change of the sense of rotation makes a significant change in the state of polarization of the emergent light.

6.6 For $k_1 = 1$ and $k_2 = 0$, the direction of polarization of the emergent light from the stacked polarizers is always in the azimuth direction of the last polarizer.

(a) $\theta = \theta_2$.

(b) $\theta = \theta_1$.

6.7 The horseshoe crab sees linear polarization when it is oriented in a north–south direction. When it is oriented in other directions, the polarization is elliptical.

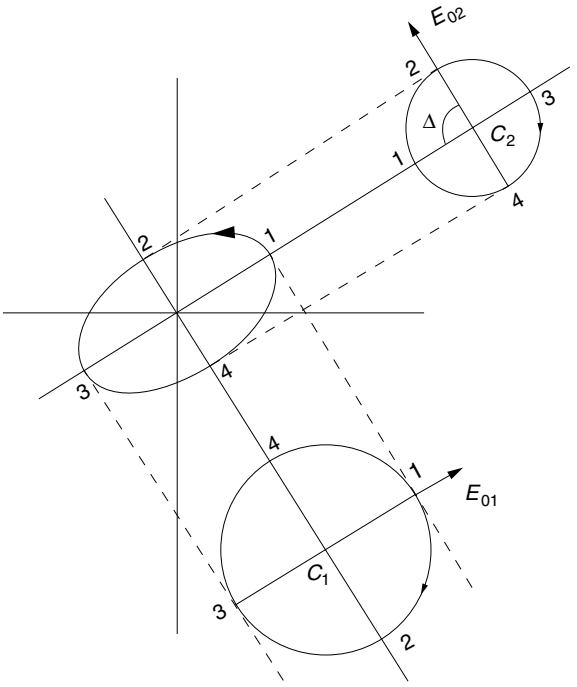

Figure A6.4 When an elliptically polarized wave is decomposed into parallel and perpendicular components, there is a 90° phase difference between the components.

To face north (or south) it turns its body until linear polarization is sensed. This can be seen from Fig. 6.33 by making these substitutions: the observer is the horseshoe crab, the light source is a ray of sunlight, and the scattering center is a particle in the water. The direction of linear polarization is perpendicular to the plane containing the horseshoe crab, the ray of sunlight, and the scattering center. The horseshoe crab sees vertically linearly polarized sunlight.

6.8 Because of the optical activity, the direction of polarization rotates. Wherever the light is horizontally polarized, no scattered light propagates horizontally because the direction of the **E** field becomes parallel to the direction of propagation. This happens every 180° of rotation. If the rotary power of quartz is $[\theta]^{20^\circ\text{C}}_{0.63\ \mu\text{m}} \doteqdot 19.5$ deg/mm, the period of modulation is $L = 180/19.5 = 9.2$ mm.

6.9 Since $d_1 > d_2$, the retardance is dominated by the anisotropy of the crystal with d_1. Since the emerging light is left-handed, the polarization direction of the incident light has to be to the left of the fast axis. In other words, the fast axis is to the right of the polarization direction of the incident wave, which means the fast axis is along the optic axis in crystal d_1. The refractive index in the direction of the optic axis is n_e, while the refractive index in the direction perpendicular to the optic axis (y direction) is n_o. Hence,

$$n_e < n_o$$

and the crystal is classified as negative, as mentioned in Chapter 4.

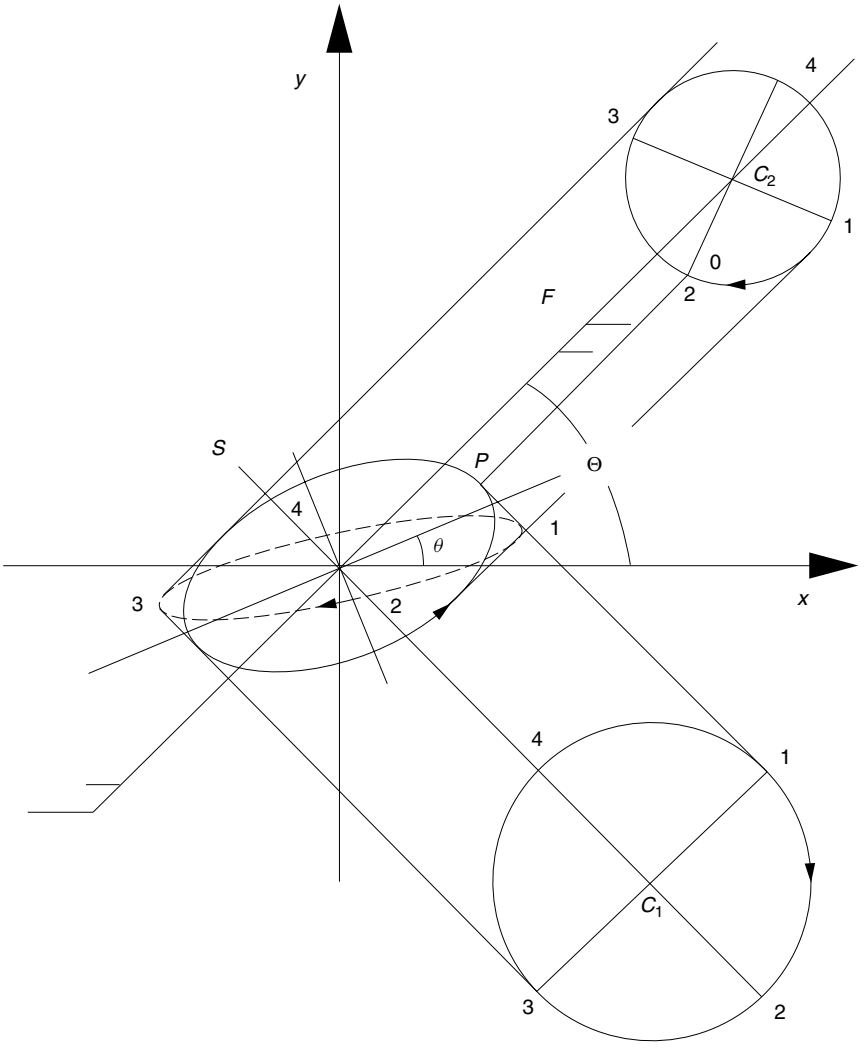

Figure A6.5 Same configuration as that shown in Fig. 6.10 but with the opposite handed rotation of the incident wave.

6.10 Insert the retarder in question between a pair of crossed polarizers. This configuration is illustrated in Fig. 6.38 with the retarder as the inserted optical element. As a precaution, if the incident wave happens to be linearly polarized, check that at least some of the incident light is getting through the first polarizer. The situation where no light passes through the first polarizer is to be avoided.

Null output from the second polarizer is obtained only when the fast and slow axes of the retarder match the direction of the polarizer principal axes. Determining which axis is the fast axis, and determining the actual value of the retardance can be done by Senarmont's method (see Section 6.4.3.3).

6.11 First, the solution is obtained by circle diagrams. Partition the retardance in equal proportions between the E_x and E_y component fields. If $\Theta = 0$, delay E_y

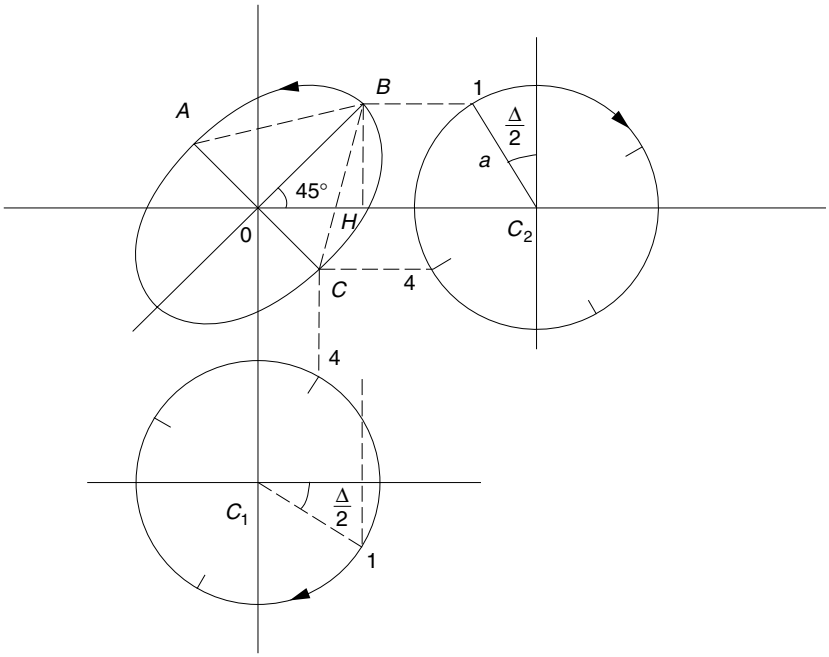

(a)

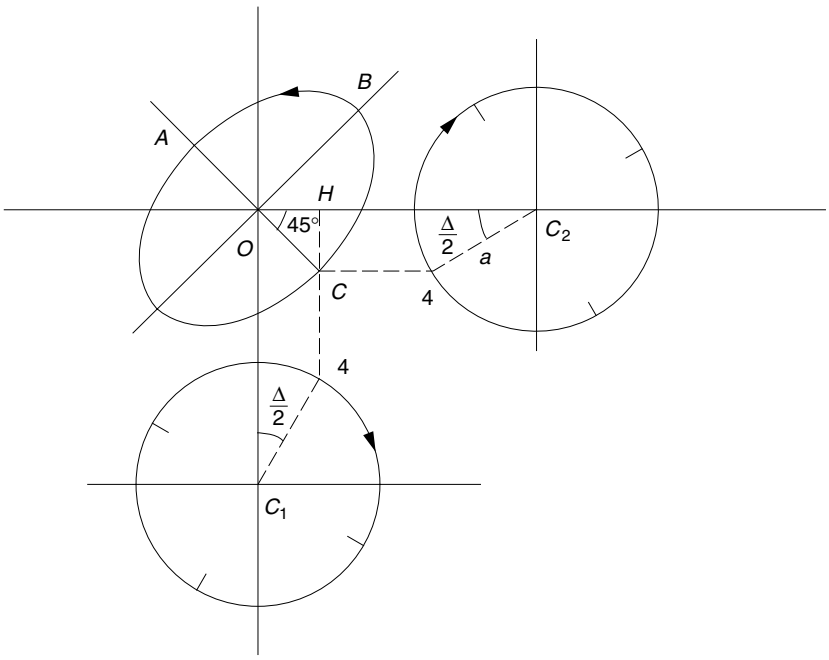

(b)

Figure A6.11 Circle diagrams. (a) Point 1 on phasors representing point *B* on the ellipse. (b) Point 4 on phasors representing point *C* on the ellipse.

by $\Delta/2$ while advancing E_x by $\Delta/2$, and draw circle diagrams as shown in Fig. A6.11(a). Points 1 on C_1 and C_2 are extended to point B on the ellipse. Point 4 on C_1 and C_2 is extended to point C on the ellipse. If we find the lengths $\overline{0B}$ and $\overline{0C}$ on the ellipse in terms of Δ, the angle $\angle ABC$ can be found in terms of Δ. From the diagram in Fig. A6.11a, we have

$$\overline{BH} = a\cos\frac{\Delta}{2}$$

As we learned from Fig. 6.4, the major and minor axes are at either $\theta = 45^\circ$ or $\theta = 135^\circ$, when $B/A = 1$, and

$$\overline{0B} = \sqrt{2}\, a\cos\frac{\Delta}{2}$$

From the diagram in Fig. A6.11b, we have

$$\overline{CH} = a\sin\frac{\Delta}{2}$$

$$\overline{0C} = \sqrt{2}\, a\sin\frac{\Delta}{2}$$

From the above two values, $\tan\beta$ is expressed as

$$\tan\beta = \frac{\overline{0C}}{\overline{0B}} = \tan\frac{\Delta}{2}$$

Finally,

$$2\beta = \Delta$$

Next, the result is obtained simply using Eq. (6.127) with $\theta = 45^\circ$. The answer is $2\beta = \Delta$.

6.12 **(a)** Note from Eqs. (6.95) and (6.98) that

$$\tan 2\alpha = \frac{2AB}{A^2 - B^2}$$

Use of Eq. (6.99) to find $\cos 2\theta$ to put into Eq. (6.123) leads to

$$(a^2 - b^2)\sin 2\theta = 2AB\cos\Delta$$

(b) Applying the identity

$$\cos 2\alpha = \frac{1 - \tan^2\alpha}{1 + \tan^2\alpha}$$

to Eq. (6.91) gives

$$\cos 2\alpha = \frac{A^2 - B^2}{A^2 + B^2}$$

Using Eq. (6.123) to find a substitute for the numerator in the above expression gives the result

$$(a^2 - b^2)\cos 2\theta = (A^2 + B^2)\cos 2\alpha$$

Chapter 7

7.1 The diagram is shown in Fig. A7.1. The emergent wave is a right-handed elliptically polarized wave with

$$\epsilon = 0.2 \quad \text{and} \quad \theta = 80^\circ$$

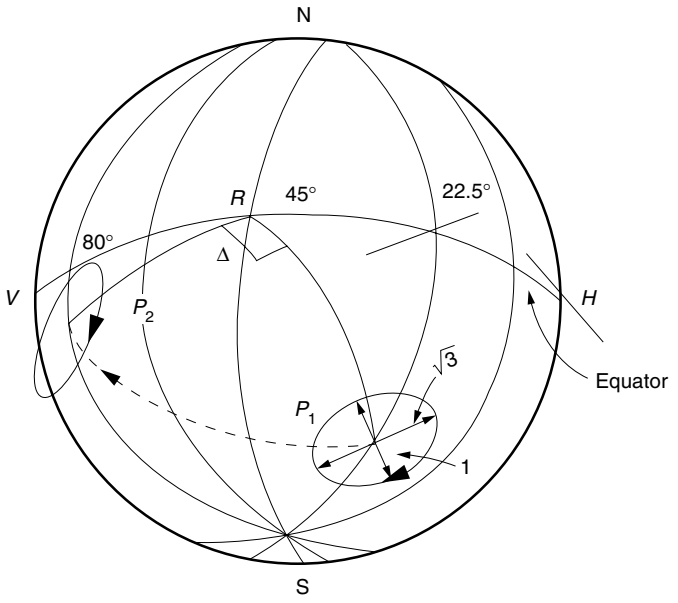

Figure A7.1 Solution of Problem 7.1.

7.2 The answers are shown in Fig. A7.2.

7.3 Figure A7.3 shows the geometry of the antiglare screen. Incident white light is first converted into a vertically polarized wave, which can be represented as P_1 on the Poincaré sphere. The azimuth Θ of the fast axis of the $\lambda/4$ sheet is 45°, which is represented by R on the Poincaré sphere. The incident point P_1 is rotated by 90° around R to P_2 at the north pole. Thus, the incident wave to the radar screen is a left-handed circularly polarized wave.

The radar screen reflects the incident light. The direction of rotation of the reflected circularly polarized wave is the same as that of the incident wave on the radar screen, but the direction of the propagation reverses and the reflected light looking toward the radar screen from the operator is right-handed. It is represented by the south pole on the Poincaré sphere.

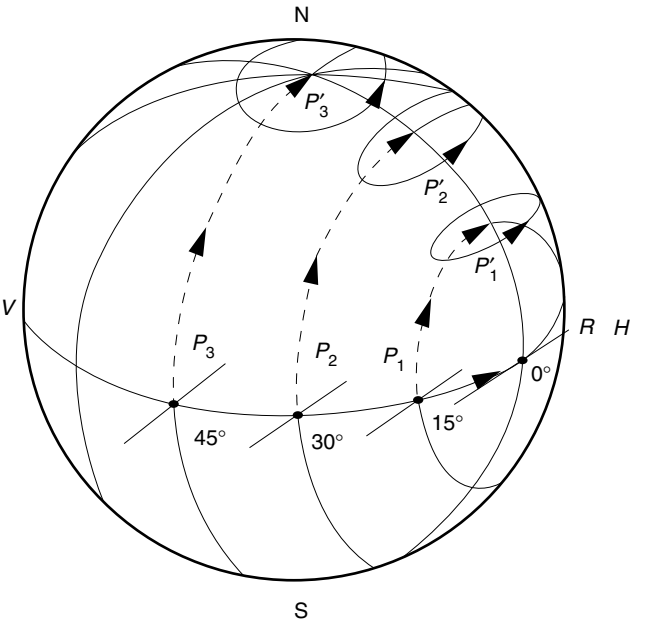

(a)

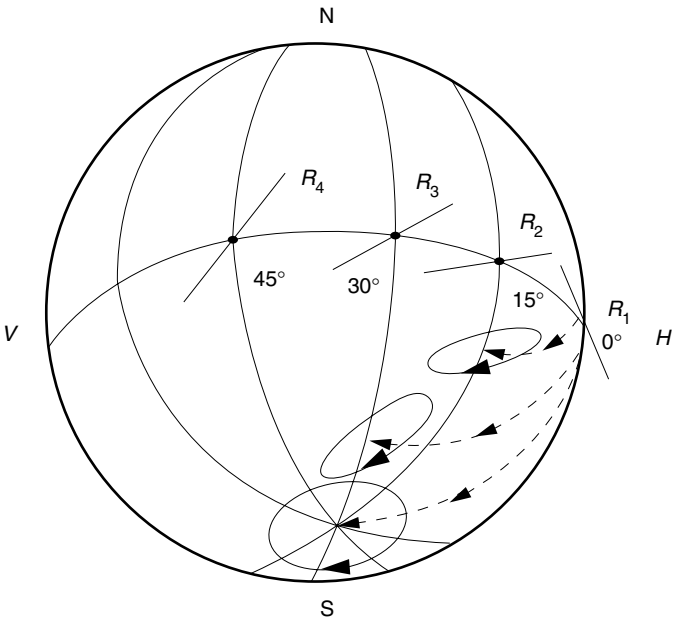

(b)

Figure A7.2 (a) Three different azimuths of incident light for a fixed $\lambda/4$ plate. (b) Three different azimuths of the fast axis of $\lambda/4$ plate for a fixed incident light.

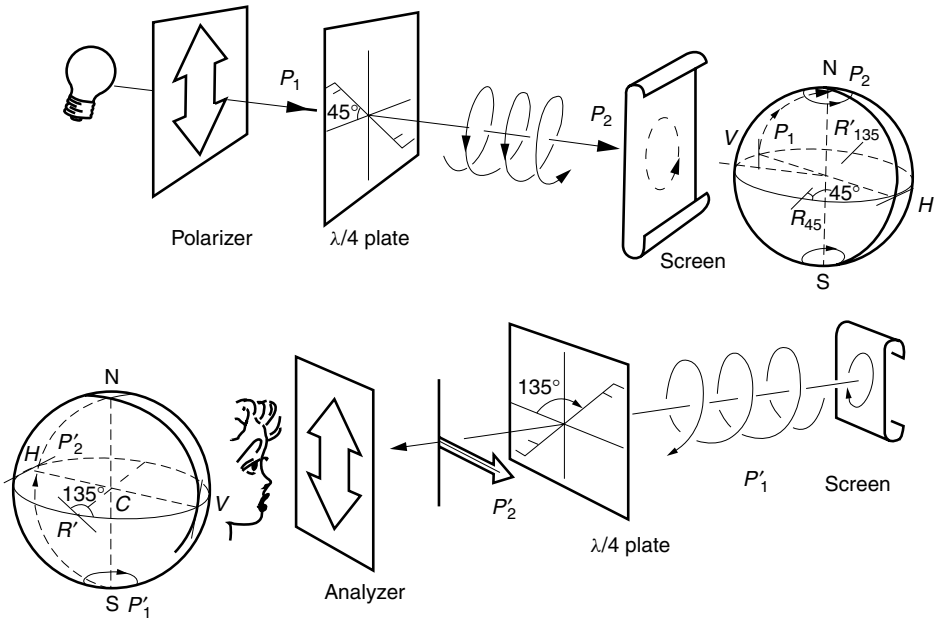

Figure A7.3 Polarization stages of an antiglare sheet plotted on the Poincaré sphere.

The azimuth of the fast axis of the same $\lambda/4$ sheet now appears at $\Theta = 135°$. The reflected light P'_1 is rotated by 90° around R' at $\theta = 135°$ to generate a horizontally linearly polarized wave, and the reflected light is blocked by the analyzer.

Light originating from the radar screen is attenuated but reaches the operator.

7.4 Point P_1 of the incident light with $\theta = 45°$ is at the midpoint between points H and V, and P_1 appears on the circumference of the circle made by the projection of the Poincaré sphere along the HV axis, as shown in Fig. A7.4.
Point P_2 of the emergent light with β is at the latitude of 2β on the Poincaré sphere.

$$\angle P_1 C P_2 = \Delta \quad \text{and} \quad \Delta = 2\beta$$

7.5 Projections onto the horizontal, frontal, and profile planes are made. The order of drawing the points in Fig. A7.5 is:

- P_1 at $2\theta_1 = 126.8°$ in the H plane.
- P_1 at $\beta = 0$ in the F plane.
- P_1 in the P plane.
- P_2 from P_1 by $\Delta = 315°$ in the P plane.
- P_2 in the H plane to find $2\theta = 137°$
- P'_2 rotated from P_2 around NS to obtain the true angle $2\beta = 34°$.

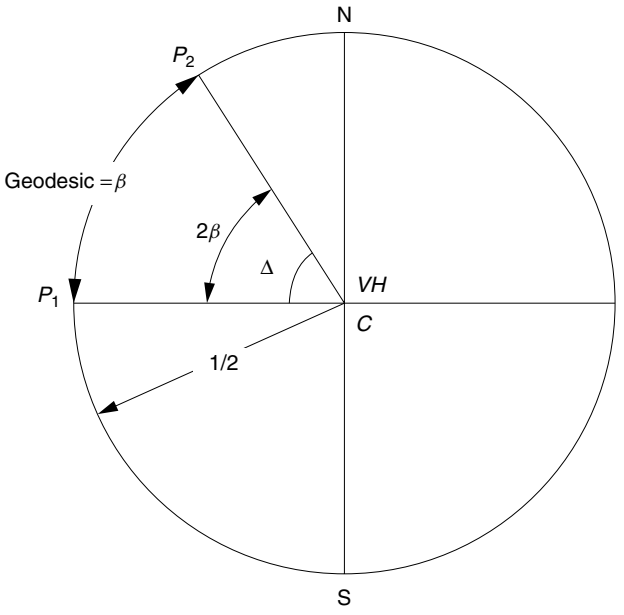

Figure A7.4 Poincaré sphere viewed along the *HV* axis.

7.6 Follow the steps explained in Example 7.12. Figure A7.6 shows the key operations. The state of the polarization of the emergent light is left-handed elliptical polarization with $(\theta, \epsilon) = (158^\circ, 0.23)$.

7.7 **(a)** The procedure is similar to that of Problem 7.5. The answers of $\theta = 60^\circ$ and $\epsilon = 0.31$ with left-handedness are verified from Fig. A7.7a.

(b) The transmittance of the analyzer is $k = \cos^2 \angle HCP_2/2$ in the upper right figure in Fig. A7.7a. The true angle is obtained when P_2 is rotated around the axis CH to the equator, so that $2\alpha = 114^\circ$ and $\alpha = 57^\circ$. The transmitted power intensity P_t is

$$P_t = \frac{\eta_0}{2}(E_x^2 + E_y^2)\cos^2 57^\circ = 2.0\eta_0 \text{ W/m}^2$$

(c) The answer is in Fig. A7.7b:

$$2\alpha = 74^\circ \quad \text{and} \quad k = \cos^2 \alpha = 0.64$$

7.8 The operation is quite similar to that of Example 7.13. The major difference is the bipolar nature of the external field ε_x. As shown in Fig. A7.8a the solid line indicates the shape of the indicatrix when the external field is $+\varepsilon_x$. The indicatrix is rotated as shown by the dotted line when the external field is changed to $-\varepsilon_x$. The direction of the fast axis rotates by 2θ, when the polarity of ε_x is reversed. Thus, the azimuth Θ of the fast axis is alternately at R and R' on the Poincaré sphere. The amount of retardance Δ is the same for both.

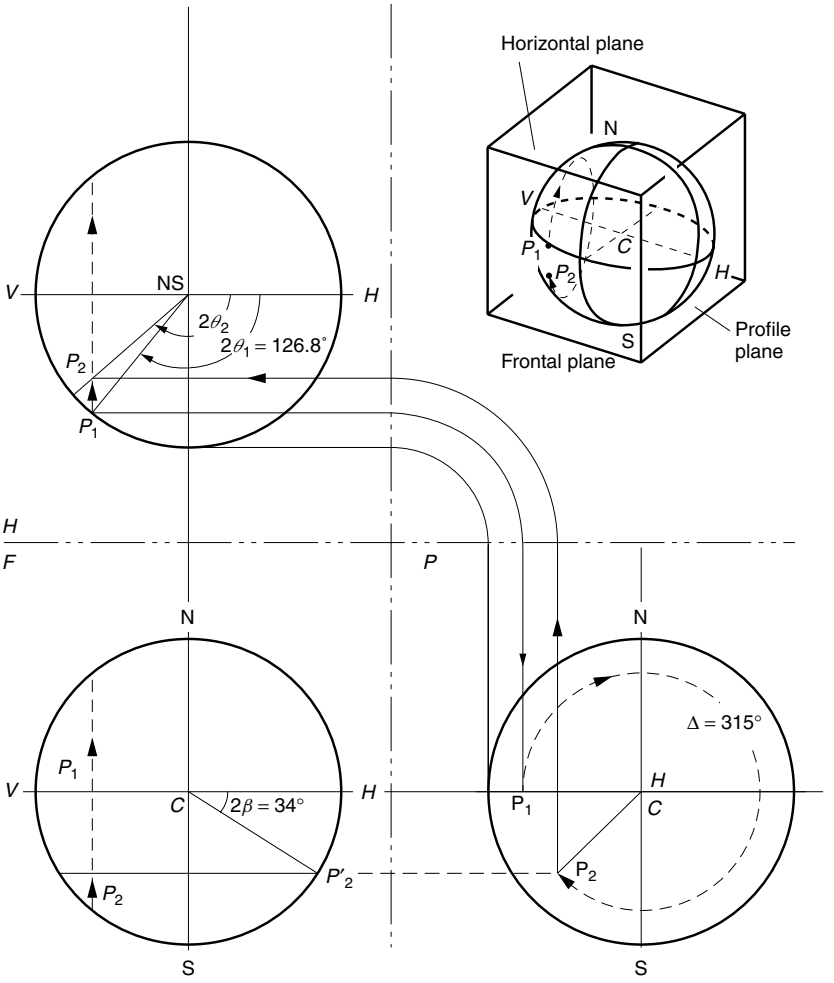

Figure A7.5 Finding θ and β Poincaré sphere traces.

With this TE–TM converter, the retardance of the modal retarder is 180° so that the spiral locus on the Poincaré sphere moves toward point V as the light passes through the interdigital electrodes, as shown in Fig. A7.8b.

The incident light P_1 is first rotated around R by Δ to P_2 by the first conversion retarder. The first modal retarder rotates point P_2 by 180° around the HV axis to P_3. The fast axis of the second conversion retarder, however, is moved to $+\theta$ and P_3 is rotated around R' rather than around R by Δ to P_4. The second modal retarder rotates by 180° from P_4 to P_5 around point H.

The same procedure repeats, and the point moves toward point V.

7.9 Let the two oppositely propagating beams be represented by

$$\begin{aligned} E_x &= Ae^{j\beta z - j\omega t} \\ E_y &= Be^{-j\beta z - j\omega t} \end{aligned} \tag{1}$$

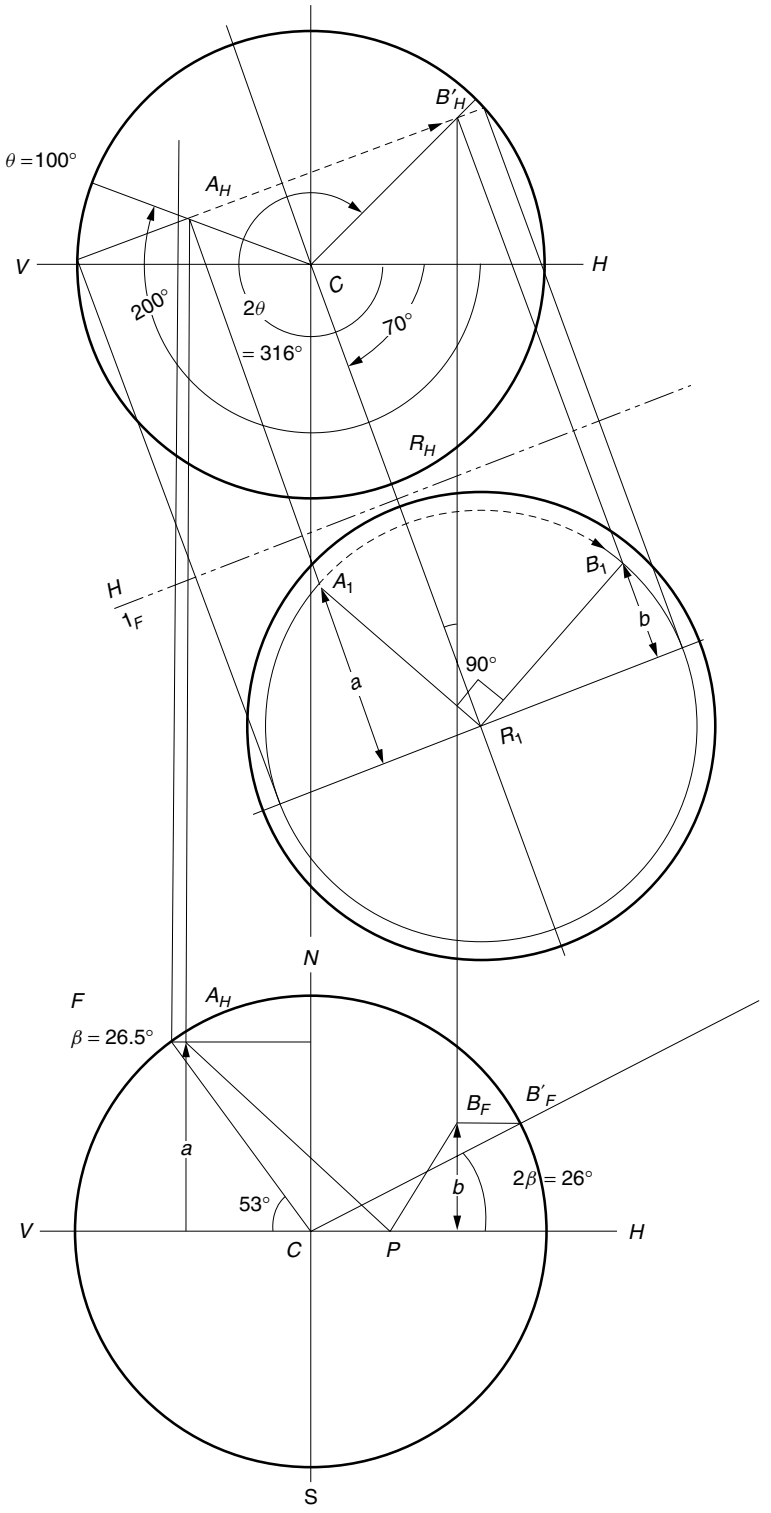

Figure A7.6 Solution by Poincaré sphere traces.

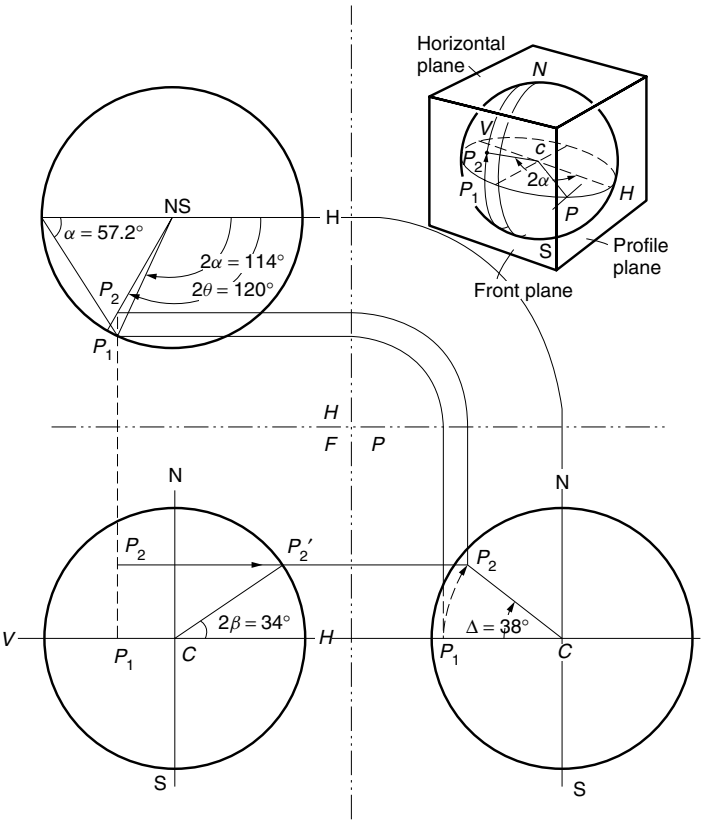

(a)

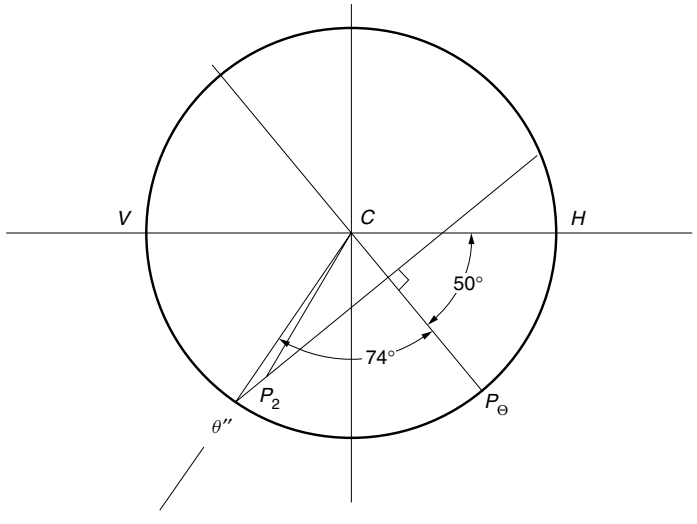

(b)

Figure A7.7 Solution of Problem 7.7. (a) Finding θ and β by Poincaré sphere trace. (b) Finding the transmittance of an analyzer with $\Theta = 25^\circ$.

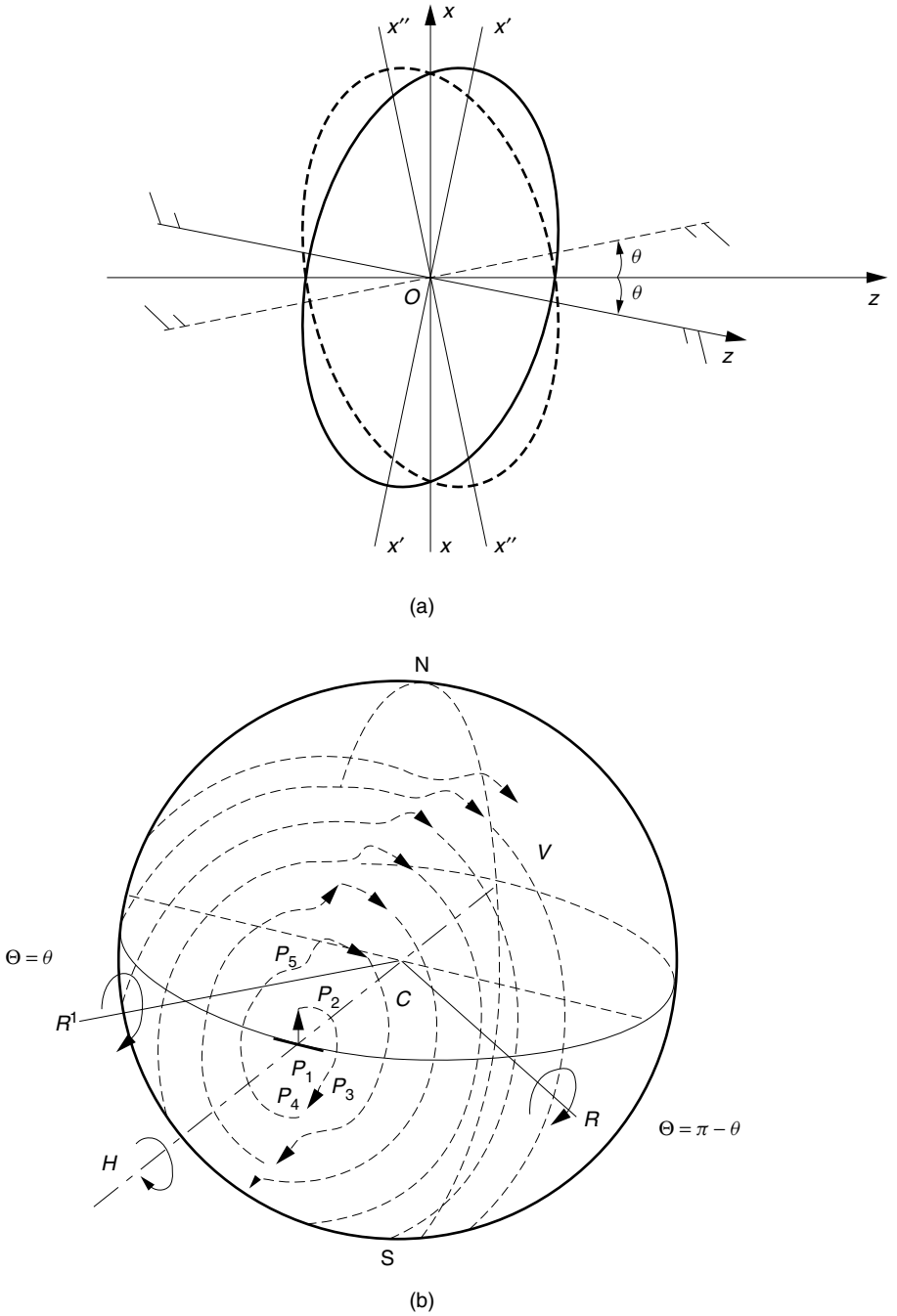

Figure A7.8 Solution of Problem 7.8. (a) Indicatrix of the optical guide. (b) Movement of the state of polarization on the Poincaré sphere.

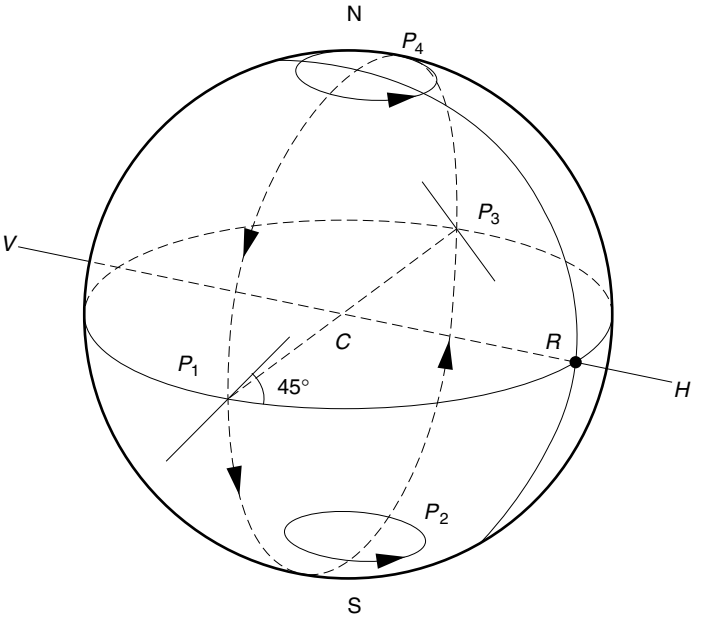

Figure A7.9 Polarization grating for laser cooling.

The component field ratio is

$$\frac{E_y}{E_x} = e^{-j2\beta z} \tag{2}$$

where $A = B$ (or $\alpha = 45^\circ$) is assumed. Equation (2) is equivalent to a retarder whose fast axis is along the x axis and whose retardance is

$$\Delta = -2\beta z \tag{3}$$

The distribution of the state of polarization along the z axis is found using the Poincaré sphere in Fig. A7.9. P_1 represents linearly polarized light with $\theta = 45^\circ$ at $z = 0$. As z is increased P_1 rotates by $-2\beta z$ (counterclockwise) on the Poincaré sphere with point H as its center of rotation. The state of polarization changes in the following order: linearly polarized at $\theta = 45^\circ$, right-handed circularly polarized, linearly polarized at $\theta = 135^\circ$, left-hand circularly polarized, and so on, at every $\Delta z = \lambda/8$.

Chapter 8

8.1 There is a time lapse $\tau = 2L/c$ between the two entries of the incident and reflected waves into the distorting medium. The distortion-free image is recovered when

$$\Phi(t) = \Phi(t - \tau)$$

$\Delta\Phi = \Phi(t) - \Phi(t-\tau)$ can be used as a criterion for the quality of the recovered image:

$$\begin{aligned}\Delta\Phi &= \Phi_0[\cos\omega t - \cos\omega(t-\tau)] \\ &= \tfrac{1}{2}\Phi_0 \sin(\omega\tau/2)\cos\omega(t-\tau/2)]\end{aligned}$$

If $\Delta\Phi$ is zero, the best image is recovered; that is, when

$$\omega\frac{\tau}{2} = n\pi \quad \text{or} \quad \frac{2L}{c} = nT$$

where T is the period of the fluctuation. This happens when the return-trip time matches the fluctuation period and the wave sees the same fluctuation on both trips. The worst case is when

$$\frac{2L}{c} = \frac{2n+1}{2}T$$

The wave that saw the maximum Φ on the initial trip sees the minimum on the return trip, and the worst recovery is made.

8.2 **(a)** Although the atoms are symmetric with respect to position, they are not symmetric with respect to the polarity of the charges; therefore, the crystal does not possess inversion symmetry.

(b) The redistributed charges are shown in Figs. A8.2a and A8.2b for $\mathbf{E} = E\hat{\mathbf{x}}$ and $\mathbf{E} = -E\hat{\mathbf{x}}$. The amount of polarization is different when the direction of $\mathbf{E}$ is reversed, and the polarization with respect to time is as shown in Fig. A8.2c.

(c) Since the curve for positive values of P_{NL} is different from that of negative P_{NL}, the second order nonlinearity can exist. The addition of the fundamental and the second harmonic in Fig. A8.2d conforms with that in Fig. A8.2c.

8.3 The curve of P_{NL} for the crystal with inversion symmetry should have the same shape for positive P_{NL} and negative P_{NL}, as indicated in Fig. A8.3a. If the fundamental and the fourth order harmonic in Fig. A8.3b are added, the result is as shown in Fig. A8.3c. The shape of positive P_{NL} is not the same as that of negative P_{NL} and cannot conform with the curve in Fig. A8.3a. Thus, $\chi^{(4)} = 0$.

8.4

$$\begin{aligned}\mathbf{P}_{\text{NL}} = \hat{\mathbf{x}}\epsilon_0\chi_{xxxx}[&A_1\cos(k_1z - \omega t + \phi_1) \\ &+ A_2\cos(k_2z - \omega t + \phi_2) + A_3\cos(k_3z - \omega t + \phi_3)]^3 \qquad (1)\end{aligned}$$

Put

$$\begin{aligned}a &= A_1 e^{j(-\omega_1 t + k_1 z + \phi_1)} \\ b &= A_2 e^{j(-\omega_2 t + k_2 z + \phi_2)} \qquad (2) \\ c &= A_3 e^{j(-\omega_3 t + k_3 z + \phi_3)}\end{aligned}$$

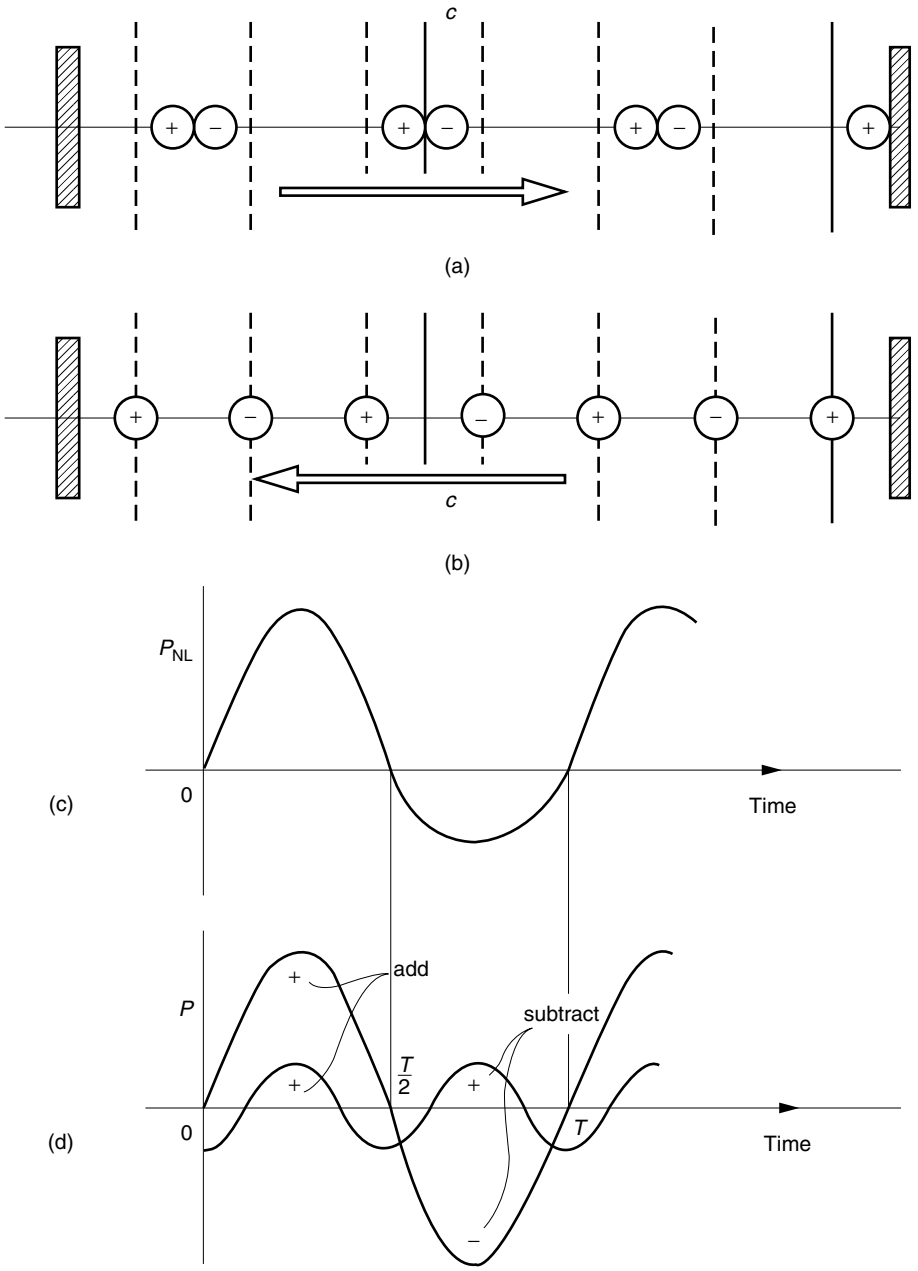

Figure A8.2 Proof of nonzero $\chi^{(2)}$. (a) Charge distribution for $E = E\hat{\mathbf{x}}$. (b) Charge distribution for $E = -E\hat{\mathbf{x}}$. (c) P_{NL} as a function of time. (d) Addition of fundamental and second harmonic.

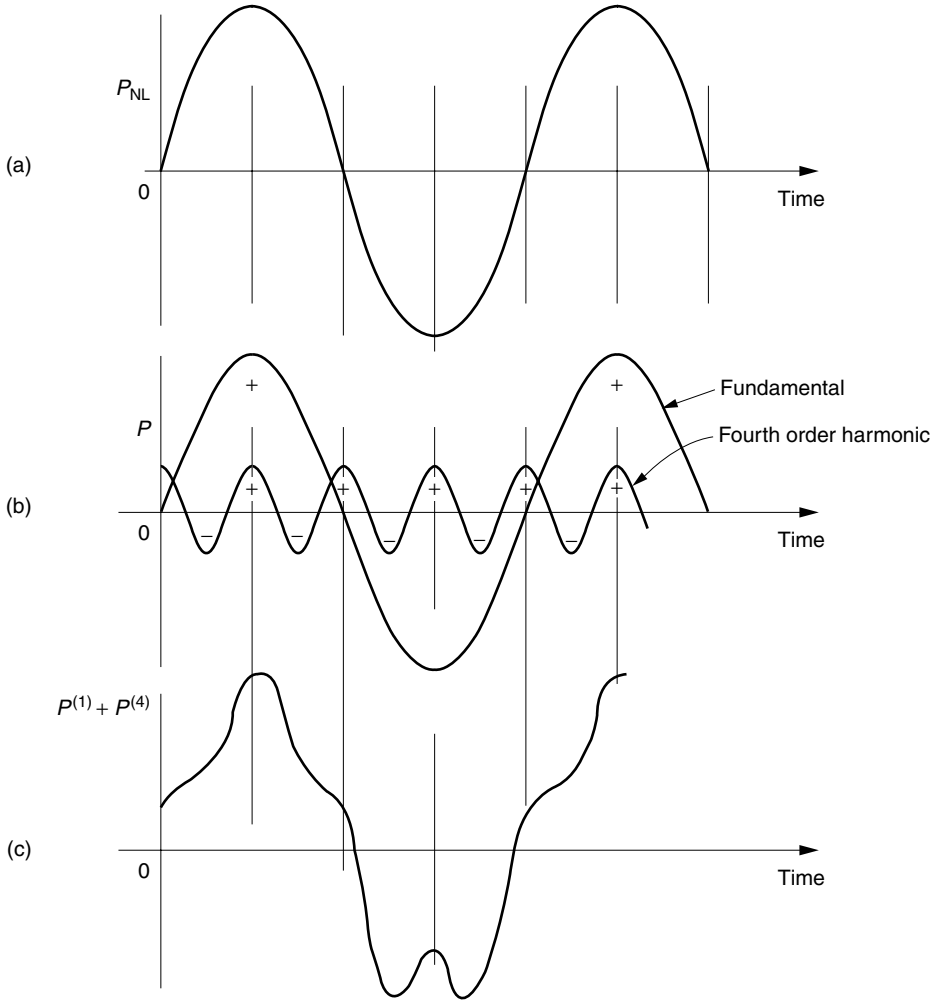

Figure A8.3 $\chi^{(4)} = 0$ for a crystal with inversion symmetry.

Then, Eq. (1) becomes

$$\mathbf{P}_{\mathrm{NL}} = \hat{\mathbf{x}}\epsilon_0 \chi_{xxxx} \tfrac{1}{8}(d + d^*)^3 \tag{3}$$

where

$$d = a + b + c \tag{4}$$

which is reduced to

$$P_{\mathrm{NL}} = \frac{\epsilon_0}{8}\chi_{xxxx}(d^3 + 3d^2 d^* + \text{c.c.}) \tag{5}$$

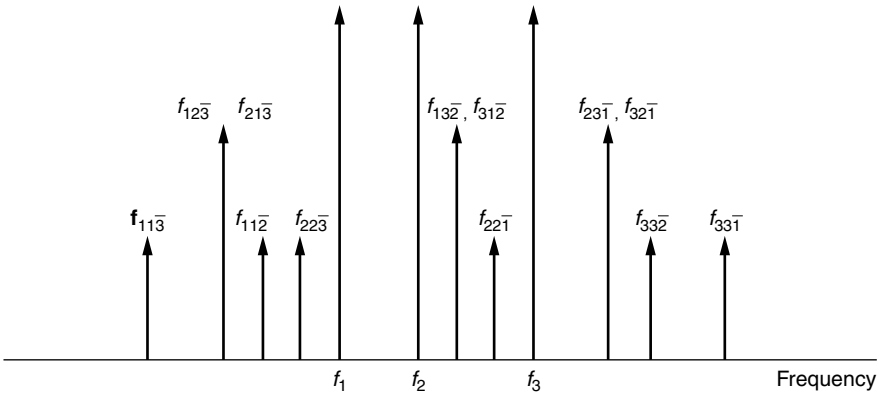

Figure A8.4 Spectra generated due to $\chi^{(3)}$ of the optical fiber. For instance, $f_{23\bar{1}} = f_2 + f_3 - f_1$.

Frequencies associated with d^3 are too high and are out of the range of interest. Discarding these terms gives

$$P_{\mathrm{NL}} = \frac{3\epsilon_0}{8}\chi_{xxxx}(d^2 d^* + \text{c.c.}) \tag{6}$$

Insertion of Eq. (4) into Eq. (6) generates many terms and the calculated result is

$$\begin{aligned}\frac{8P_{\mathrm{NL}}}{3\epsilon_0\chi_{xxxx}} &= a(|a|^2 + 2|b|^2 + 2|c|^2) \\ &\quad + b(2|a|^2 + |b|^2 + 2|c|^2) \\ &\quad + c(2|a|^2 + 2|b|^2 + |c|^2) \\ &\quad + b^2a^* + c^2a^* + a^2b^* + c^2b^* + a^2c^* + b^2c^* \\ &\quad + bca^* + cba^* + acb^* + cab^* + abc^* + bac^* + \text{c.c.}\end{aligned} \tag{7}$$

For instance, frequency component of b^2a^* is, from Eq. (2), $2\omega_2 - \omega_1$ and that of bca^* is $\omega_2 + \omega_3 - \omega_1$. There are 15 frequencies, of which 3 are redundant in the last 6 terms, for a total of 12 different frequencies, as shown in Fig. A8.4.

After going through the fiber, the three input frequencies have generated 12 output frequencies. Stimulated Brillouin scattering in the glass is the main contributor to the third order nonlinearity. This, sometimes, does harm and creates serious crosstalk problems among highly wavelength division multiplexed channels and prevents the use of high-intensity light in this type of optical communication system [25].

8.5 In order to sustain four-wave mixing, both the frequency (Eq. (8.54)) and phase (Eq. (8.70)) matching conditions must be met. Since all frequencies are identical, Eq. (8.54) is satisfied. Since the magnitudes of all vector propagation constants are identical, the tips of the propagation vectors lie on the circumference of the same circle. The vector $\mathbf{k}_1 + \mathbf{k}_2$ has to be identical to $\mathbf{k}_3 + \mathbf{k}_4$. As shown in

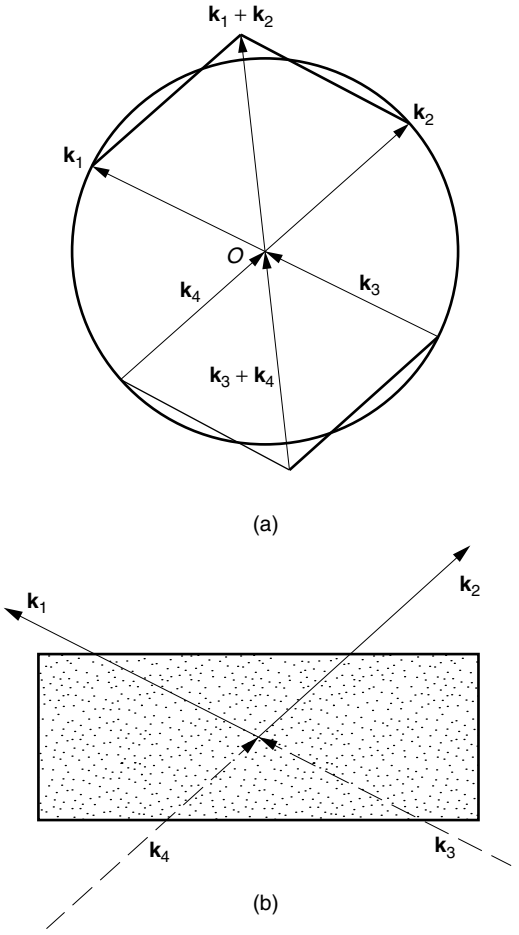

Figure A8.5 Conditions to sustain four-wave mixing. (a) Phasor diagram of **k** vectors. (b) Directions of $\mathbf{k}_3$ and $\mathbf{k}_4$.

Fig. A8.5, the only possible combination is for $\mathbf{k}_3$ to be identical to $\mathbf{k}_1$ (or $\mathbf{k}_2$), and for $\mathbf{k}_4$ to be identical to $\mathbf{k}_2$ (or $\mathbf{k}_1$).

8.6 There are six combinations, but two are redundant. There are four different patterns altogether, as shown in Fig A8.6.

8.7 The first equation is rewritten as

$$\frac{dA_p}{dz} = \gamma A_p$$

with $\gamma = j\beta_p - \alpha$. The solution of this equation is

$$A_p = A_p(0)e^{\gamma z}$$

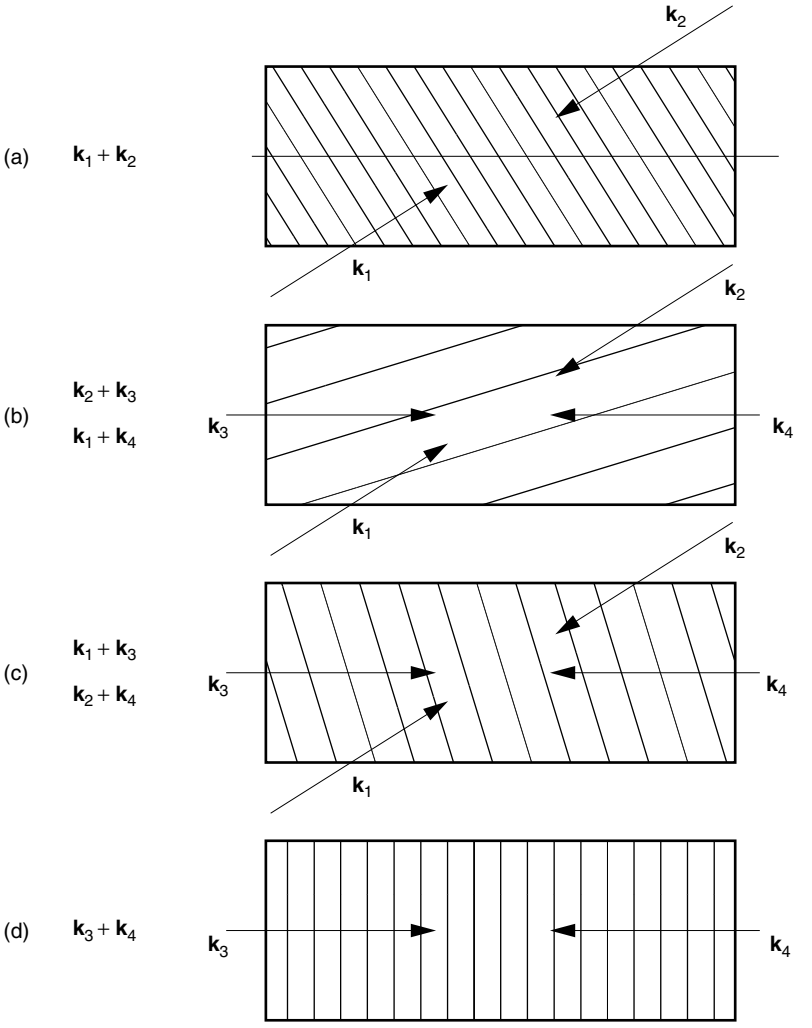

Figure A8.6 Fringe patterns generated by various combinations of two waves.

Next, the other two equations are simplified by letting

$$A_s = A_{s0}e^{\gamma z}$$
$$A_c = A_{c0}e^{\gamma z}$$

The result is

$$\frac{dA_{s0}}{dz} = jKA_p^2(0)A_{c0}^*$$
$$\frac{dA_{c0}}{dz} = jKA_p^2(0)A_{s0}^*$$